Chapter 6

RESULTS AND ANALYSIS

6.1.General

The intact pillars (including barriers) and remnant pillars are the critical elements of a mechanized depillaring panel, and the stability of these elements depicts the success of the depillaring operation. The stability of the intact pillars and remnant pillars have been accessed in the study for different geo-mining conditions using numerical simulation techniques. Panels of sufficiently large size have been prepared in the study and simulated for different combinations of pillar widths and depths. The simulation results have been obtained in terms of the vertical stress and the yield profile of the panel. The maximum depth up to which the panel is stable has been determined for each selected pillar. The panels have been further simulated to obtain optimum remnant pillar design for each selected pillar. The working pillar has been extracted in the panel by adopting suitable extraction patterns. The panel (including remnant pillars) has been simulated again at a critical depth of cover for designing the remnant pillars. The optimum remnant pillar design has been obtained for each selected pillars by varying the size of the snook. The stable cases of the panels satisfying the design criteria have been chosen for the analysis. Guidelines have been prepared to design the panel of bord and pillar system for mechanized depillaring.

6.2.Panel design

The stability of the pillars during depillaring is always required for a smooth mining operation. The maximum vertical stress arises on the pillars nearby goaf, mainly

working and barrier pillars (which have been surrounded by the goaf from both sides) at a depillaring stage where advancement length is equivalent to the panel width. The working and barrier pillars (surrounded by goaf from both sides) are the critical elements of a mechanized depillaring panel. The stability of these focused pillars (working/barrier) at a critical depillaring stage has been accessed for different pillar widths and depths using numerical simulation techniques. Four different pillars have been selected for the study, i.e., pillar width of 26 m, 35 m, 45 m, and 48 m. The panels formed by these pillars have been simulated at different depths of cover ranging from 90 m to 450 m (with an interval of 30 m). The simulation results were obtained in terms of vertical stress profile and yield profile at the mid-level of the pillars. The *FOS* of the focused pillars (working and barrier pillar) has been evaluated for all the cases of the panels. The average vertical stress on the focused pillars has been obtained using the *FISH* function of *FLAC*^{3D}. The strength of each pillar was determined separately by obtaining its stress-strain curve using numerical techniques. The stable cases of the panel satisfying the design criteria have been chosen for the analysis. The simulation results of the unstable cases have been provided in Appendix – B.

6.2.1. Simulation results for pillar width of 26 m

The panel with a pillar width of 26 m has been simulated for a depth range of 90 m – 150 m. The simulation results have been obtained in terms of vertical stress profile and yield profile. The average vertical stress on the focused pillars has been determined through *the FISH* function of *FLAC*^{3D}. The pillar strength has been determined separately using the numerical technique (i.e., 12.5 MPa). The *FOS* of the focused pillars has been determined for all the cases of the panels. The stable cases of the panel satisfying the design criteria have been discussed in this section.

a) Depth of cover: 90 m

The simulation results show that the panel is stable at a depth of 90 m and fulfills the design criteria. Fig. 6.1 shows the vertical stress and yielding profile of the panel at the mid-level of the pillars. The dark color (blue) indicates a high-stress value in the panel, whereas the light color (like yellow) shows low-stress values. The vertical stress on the pillars near to goaf edge is higher than the pillars far from the goaf edge, as seen from Fig. 6.1. The yielding of the pillar near the goaf edge is more than the far end pillar. The pillars side facing the goaf shows a yielding of about 4 m. The influence of the goaf has been observed up to one pillar from the goaf edge.

The yielding profile shows that the yielding on the working pillar ‘W’ is asymmetric. More yielding has been observed on the sides facing the goaf. On average, the working pillar yields about 4.0 m from the sides, i.e., about 65% of the pillar area. The maximum stress value has been observed 5 m – 6 m inside the pillar, i.e., about 25 MPa. Average vertical stress on the working pillars (i.e., 'W') has been computed as 9.5 MPa. The *FOS* of the working pillar in this scenario is 1.3. It has been observed from Fig. 6.1 that the barrier pillars have been yielded considerably with a small zone of the elastic core. The maximum stress value of about 25 MPa has been observed on the barrier pillars (B1 – B4). It has been observed from Fig. 6.1 that barrier pillar ‘B2’ is the most critical pillar in the panel. The average vertical stress on pillar ‘B2’ has been observed as 11.6 MPa. The *FOS* of the pillar ‘B1’ has been calculated as 1.1. It has further been observed that barrier pillar 'B6' has comparatively less stressed than the others as the presence of the intact pillars of the active panel. The average vertical stress value on pillar 'B6' has been observed as 6.1 MPa.

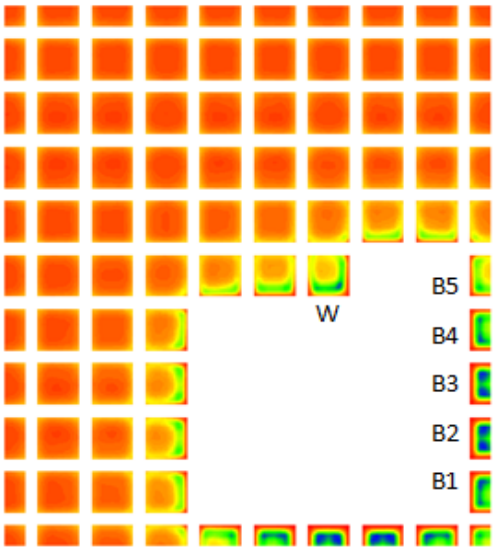

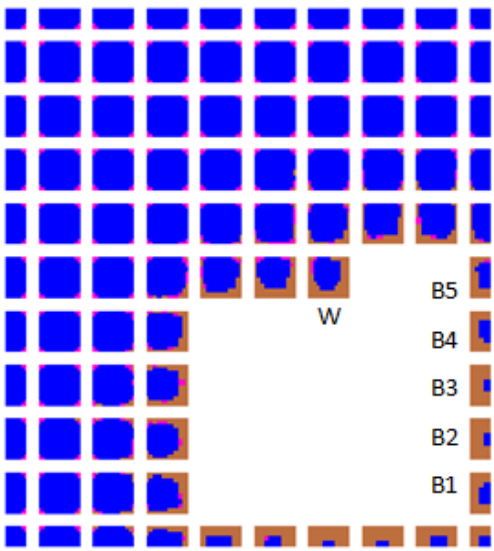

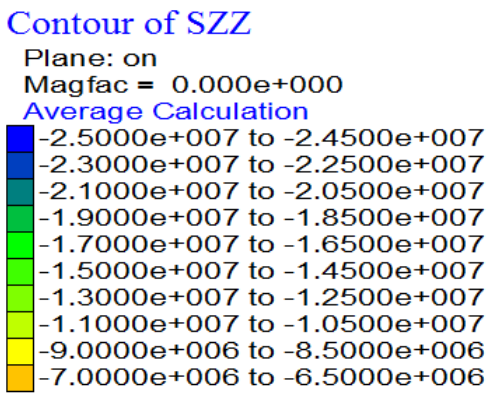

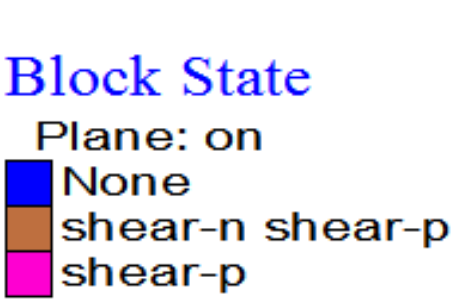

Vertical stress scale (stress in Pa)	Yielding state scale

Fig. 6.1 Vertical stress and yield profile of the panel with a pillar width of 26 m at a depth of 90 m

The pillars away from the goaf edge show a symmetrical stress distribution. The pillar 'F,' which is at a far-end from the goaf, experiences a vertical stress value of about 3.6 MPa, equivalent to the stress at the development stage (i.e., 3.8 MPa). The *FOS* of the far-end pillar (‘F') has been calculated as 3.5. Table 6.1 shows the simulation results of the panel concerning the focused pillars.

Table 6.1 Simulation results of the panel with a pillar width of 26 m at a depth of 90 m

Pillar/Barrier No.	Average stress on pillar (MPa)	Yield percentage (%)	FOS
W	9.5	65	1.3
B1	11.6	80	1.1
B2	11.6	90	1.1
B3	11.5	90	1.1
B4	11.3	80	1.1
B5	9.3	70	1.4
B6	6.1	10	2.0
F	3.6	5	3.5

b) Depth of cover: 120 m

The panel having a pillar width of 26 m does not satisfy the design criteria at a depth of 120 m. The panel completely fails during the simulation process. The vertical stress and yielding profile of the panel at a depth of 120 m (before complete failure) have been provided in Appendix – B1.

The panel has not been further simulated for the depth of 150 m, considering the simulation results at a depth of 120 m.

6.2.2. Simulation results for pillar width of 35 m

The panel with a pillar width of 35 m has been simulated for a depth range of 150 m – 240 m. The simulation results were obtained in terms of vertical stress profile and yield profile. The average vertical stress on the focused pillars has been determined through *the FIS*H function of *FLAC*^{3D}. The pillar strength has been determined separately using the numerical technique (i.e., 17.0 MPa). The FOS of the focused pillars (working/barrier) has been determined at a critical depillaring stage for different depths. The stable cases of the panel satisfying the design criteria have been discussed in this section.

a) Depth of cover: 150 m

The simulation results show that the panel is stable at a depth of 150 m and fulfills the design criteria. Fig. 6.2 shows the vertical stress and yielding profile of the panel at the mid-level of the pillars. The dark color (blue) indicates a high-stress value on the pillars, whereas the light color (like yellow, orange) shows a low-stress value. It has been observed that the vertical stress on the pillars near to goaf edge is higher than the pillars far from the goaf edge. The influence of the goaf has been observed up to one pillar from the goaf edge. It has been observed from Fig. 6.2 that the barrier pillars have been yielded considerably with a small zone of the elastic core. The maximum stress value of about 30 MPa has been observed on the barrier pillars (B1 – B4). The barrier pillar ‘B2’ is observed to be the critical pillar that experiences average vertical stress of about 15.1 MPa. The *FOS* of the critical barrier pillar ‘B2’ has been calculated as 1.1. It has further been observed that the barrier pillar 'B6' has comparatively less stressed than the others due to the intact pillars' presence.

The average vertical stress value on pillar 'B6' has been observed as 8.4 MPa. The yielding profile shows that the yielding on the working pillar 'W' is asymmetric. More yielding has been observed on the sides facing the goaf. On average, pillar 'W' has been yielded about 60%, and the maximum stress value of about 32 MPa has been observed 5 m – 6 m inside the pillar. Average vertical stress on the working pillars (i.e., 'W') has been computed as 11.8 MPa. The *FOS* of the working pillar in this scenario is 1.4. The pillars away from the goaf edge show a symmetrical stress distribution. The pillar 'F,' which is at a far-end from the goaf, experiences a vertical stress value of about 5.2 MPa, equivalent to the stress at the development stage (i.e., 5.5 MPa). The *FOS* of the far-end pillar ('F') has been calculated as 3.5. Table 6.2 shows the simulation results of the panel concerning the focused pillars.

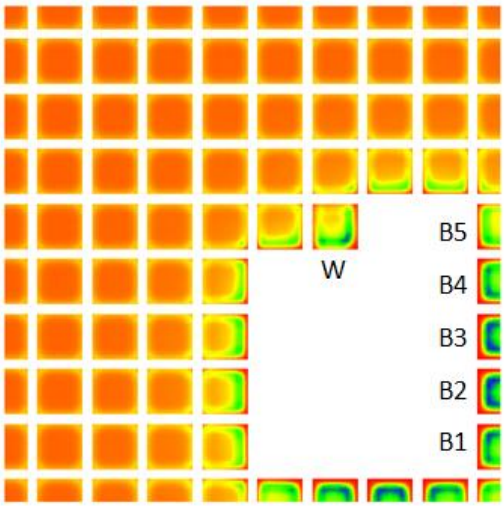

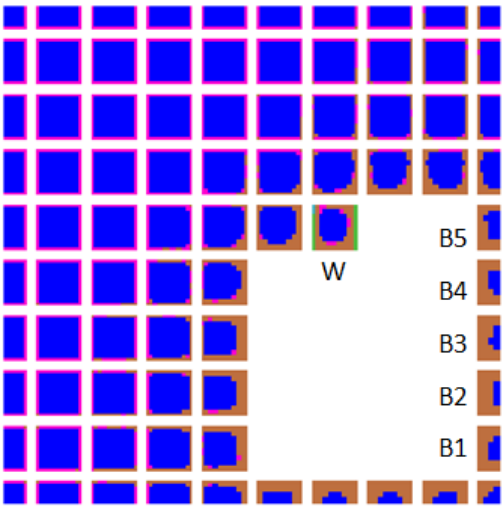

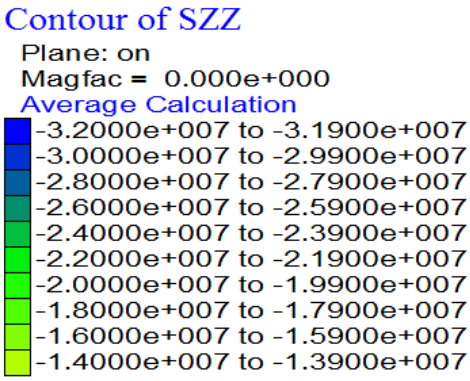

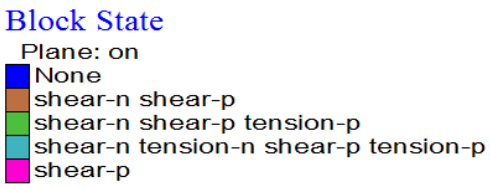

Vertical stress scale (stress in Pa)	Yielding state scale

Fig. 6.2 Vertical stress and yield profile of the panel with a pillar width of 35 m at a depth of 150 m

Table 6.2 Simulation results of the panel with a pillar width of 35 m at a depth of 150 m

Pillar/Barrier No.	Average vertical stress (MPa)	Yield percentage (%)	FOS
W	11.8	60	1.4
B1	14.6	70	1.2
B2	15.1	80	1.1
B3	15.0	75	1.1
B4	14.3	70	1.2
B5	12.2	65	1.4
B6	8.4	40	2.0
F	5.2	10	3.3

b) Depth of cover: 180 m

The panel is found to be stable at a depth of 180 m and fulfills the design criteria. Fig. 6.3 shows the vertical stress and yielding profile of the panel at the mid-level of the pillars. It has been observed from the vertical stress profile that the pillars near to goaf edge show higher vertical stress than the pillars far from the goaf edge, as indicated by the blue color in Fig. 6.3). The influence of the goaf has been observed up to one pillar from the goaf edge. The yielding profile shows that the pillar near the goaf edge has more yielded than the far end pillar (about 6 m) from the side facing the goaf.

The yielding profile shows that the yielding of the working pillar 'W' is asymmetric. More yielding has been observed on the sides facing the goaf. On average, pillar 'W' has been yielded about 7.0 m from the sides, i.e., about 65%. The maximum stress value has been observed 6 m – 7 m inside the pillar, i.e., about 40 MPa. Average vertical stress on the working pillars (i.e., 'W') has been computed as 13.1 MPa. The *FOS* of the working pillar ‘W’ has been calculated as 1.3.

It has been observed from Fig. 6.3 that the barrier pillars have been yielded considerably with a small zone of the elastic core. The maximum stress value of about 40 MPa has been observed on the barrier pillars (B1 – B4). Fig. 6.3 shows that the barrier pillar 'B2' is the most critical pillar of the panel. The average vertical stress on pillar ‘B2’ has been obtained as 16.8 MPa. The FOS of the barrier pillar ‘B2’ has been calculated as 1.0. It has further been observed that the barrier pillar 'B6' has comparatively less stressed than the others due to the presence of intact pillars. The average vertical stress value on pillar 'B6' has been observed as 10.2 MPa.

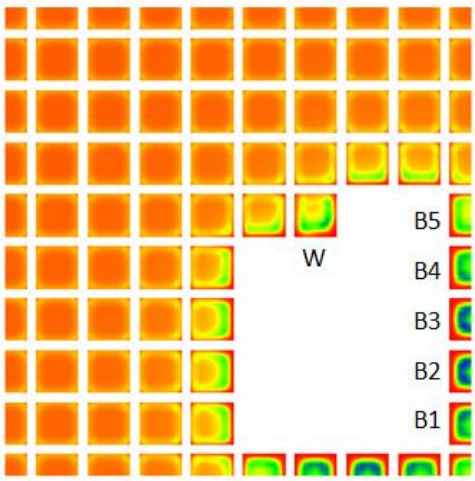

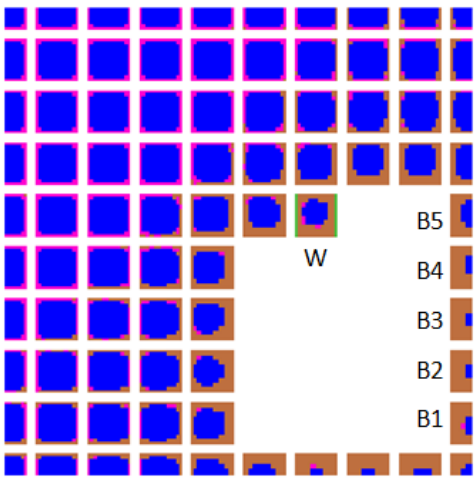

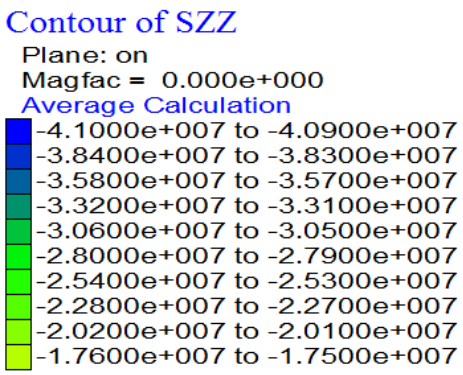

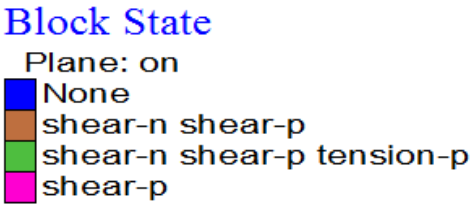

Vertical stress scale (stress in Pa)	Yielding state scale

Fig. 6.3 Vertical stress and yield profile of the panel with a pillar width of 35 m at a depth of 180 m

The pillars away from the goaf edge show a symmetrical stress distribution. The pillar 'F,' which is at a far-end from the goaf, experiences a vertical stress value of about 6.3 MPa, equivalent to the stress at the development stage (i.e., 6.5 MPa). The *FOS* of the far-end pillar (‘F’) has been calculated as 2.7. Table 6.3 shows the simulation results of the panel at a depth of 180 m.

Table 6.3 Simulation results of the panel with a pillar width of 35 m at a depth of 180 m

Pillar/Barrier No.	Average vertical stress (MPa)	Yield percentage (%)	FOS
W	13.1	65	1.3
B1	16.1	80	1.1
B2	16.8	85	1.0
B3	16.0	85	1.1
B4	15.8	80	1.1
B5	14.1	70	1.2
B6	10.20	50	1.7
F	6.3	15	2.7

c) Depth of cover: 210 m

The simulation results show that the panel is unstable at a depth of 210 m. The barrier pillars, which are surrounded by the goaf from both sides, have failed at a depth of 210 m, resulting in extreme loading conditions near the working area. The simulation results of the panel at a depth of 210 m have been provided in the Appendix – B2.

The panel has not been further simulated for the depth of 240 m, considering the simulation results at a depth of 210 m.

6.2.3. Simulation results for pillar width of 45 m

The panel with a pillar width of 45 m has been simulated for a depth range of 240 m – 360 m. The simulation results have been obtained in terms of vertical stress profile and yield profile. The dark color (blue) in the vertical stress profile shows higher stress values, whereas the light color (like yellow) shows lower stress values in the vertical stress profile. The average vertical stress on the focused pillars has been determined through *the FISH* function of *FLAC*^{3D}, whereas the pillar strength has been determined separately using the numerical technique (i.e., 26.0 MPa). The FOS

of the focused pillars has been determined for all the cases. The stable cases of the panel satisfying the design criteria have been discussed in this section.

a) Depth of cover: 240 m

The panel is stable at a depth of 240 m and fulfills the design criteria. Fig. 6.4 shows the vertical stress and yielding profile of the panel at the mid-level of the pillars. The influence of the goaf has been observed up to one pillar from the goaf edge. The vertical stress on the pillars near to goaf edge is higher than the pillars far from the goaf edge, as seen from the vertical stress profile (fig. 6.4). The yielding profile shows that the pillar near the goaf edge has more yielded than the far end pillar. The yielding of the pillars from the side facing the goaf is about 8 m.

It has been observed from Fig. 6.4 that the barrier pillars have been yielded considerably with a small zone of the elastic core. The maximum stress value of about 50 MPa has been observed on the barrier pillars (‘B1’ – ‘B4’). The barrier pillar 'B2' seems to be the most critical pillar of the panel, as seen from Fig. 6.4. The average vertical stress on the critical barrier pillar ‘B2’ has been determined as 22.8 MPa. The *FOS* of the critical barrier pillar ('B2') has been calculated as 1.1. It has further been observed that barrier pillar 'B6' has comparatively less stressed than the others due to nearby intact pillars. The average vertical stress value on pillar 'B6' has been observed as 12.5 MPa.

The yielding profile shows that the yielding on the working pillar 'W' is asymmetric. More yielding has been observed on the pillar sides facing the goaf. On average, pillar 'W' has been yielded about 7.0 m from the sides, i.e., about 60%. The maximum stress value has been observed 6 m – 7 m inside the pillar (i.e., about 35 MPa). Average vertical stress on the working pillars (i.e., 'W') has been computed as 19 MPa. The

FOS of the working pillar ('W') has been calculated as 1.4. Table 6.4 shows the simulation results of the panel at a depth of 240 m. The pillars away from the goaf edge show a symmetrical stress distribution. The pillar 'F,' which is at the far-end from the goaf edge, experiences a vertical stress value of about 7.7 MPa, equivalent to the stress at the development stage (8.0 MPa). The *FOS* of the pillar ('F') has been calculated as 2.8.

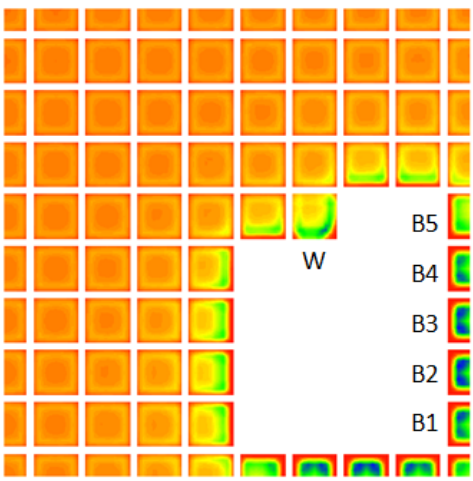

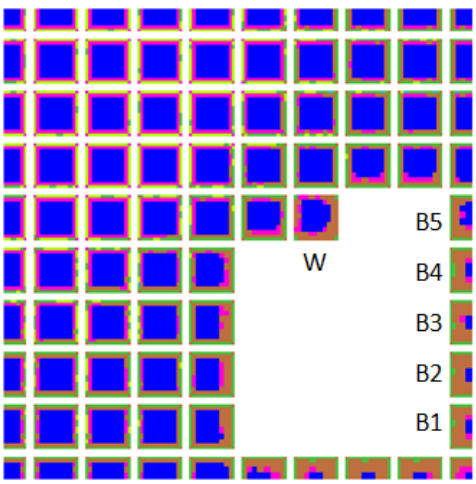

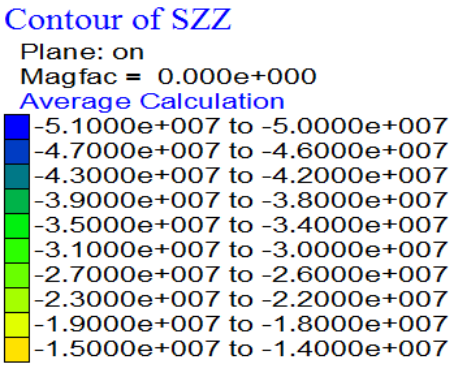

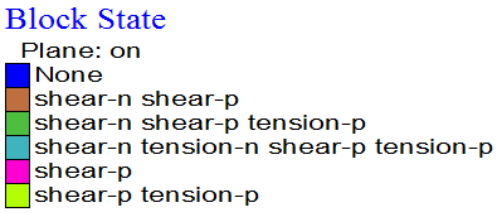

Vertical stress scale (stress in Pa)	Yielding state scale

Fig. 6.4 Vertical stress and yield profile of the panel with a pillar width of 45 m at a depth of 240 m

Table 6.4 Simulation results of the panel with a pillar width of 45 m at a depth of 240 m

Pillar/Barrier No.	Average vertical stress (MPa)	Yield percentage (%)	FOS
W	19.0	60	1.4
B1	21.1	80	1.1
B2	22.8	80	1.1
B3	22.5	80	1.1
B4	19.8	80	1.2
B5	16.4	75	1.4
B6	12.5	40	1.8
F	7.7	20	2.8

b) Depth of cover: 270 m

The panel has been observed to be stable at a depth of 270 m and fulfills the design criteria. Fig. 6.5 shows the vertical stress and yielding profile of the panel at the mid-level of the pillars. The dark color (blue) shows a higher vertical stress value, whereas, light color (yellow) shows a low stress value. The vertical stress profile shows that the pillars near to goaf edge show high vertical stress than the pillars far from the goaf edge. The yield profile shows that the pillar near the goaf edge has more yielded than the far end pillar. The yielding of the sides of the pillars facing the goaf is about 10 m. The influence of the goaf has been observed up to one pillar from the goaf edge.

The yielding of the working pillar 'W' is asymmetric. More yielding has been observed on the sides facing the goaf. On average, the working pillar 'W' has been yielded about 8.0 m from the sides, i.e., about 65%. The maximum vertical stress has been observed 7 m – 8 m inside the working pillar 'W' (i.e., about 40 MPa). The average vertical stress on the working pillars (i.e., 'W') has been computed as 19.2 MPa. The *FOS* of the working pillar 'W' has been calculated as 1.3.

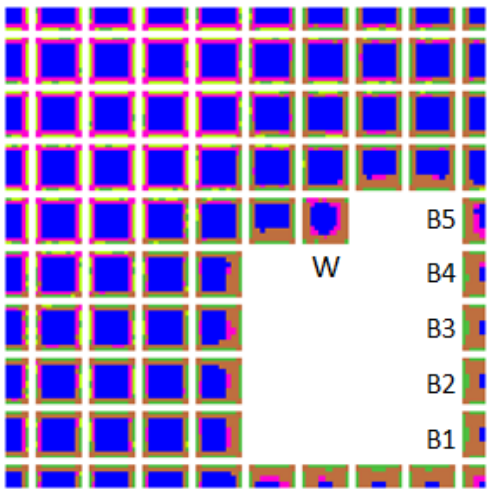

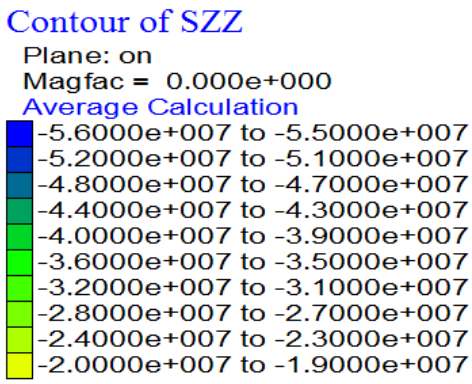

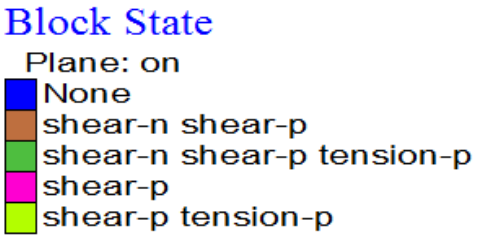

Vertical stress scale (stress in Pa)	Yielding state scale

Fig. 6.5 Vertical stress and yield profile of the panel with a pillar width of 45 m at a depth of 270 m

It has been observed from Fig. 6.5 that the barrier pillars have been yielded considerably with a small zone of the elastic core. The maximum stress value of about 55 MPa has been observed on the barrier pillars (B1 – B4). The barrier pillar 'B2' is the most critical barrier pillar of the panel and shows average vertical stress of about 23.8 MPa. The *FOS* of the critical barrier pillar 'B2' has been calculated as 1.0. It has further been observed that barrier pillar 'B6' has comparatively less stressed than the others due to the nearby intact pillars. The average vertical stress value on pillar 'B6' has been observed as 14.2 MPa. The pillars away from the goaf edge show a

symmetrical stress distribution. The pillar 'F,' which is at a far-end from the goaf, experiences a vertical stress value of about 8.8 MPa, equivalent to the stress at the development stage (9.0 MPa). The *FOS* of the far-end pillar ('F') has been calculated as 2.5. Table 6.5 shows the simulation results of the panel concerning the focused pillars.

Table 6.5 Simulation results of the panel with a pillar width of 45 m at a depth of 270 m

Pillar/Barrier No.	Average vertical stress (MPa)	Yield percentage (%)	FOS
W	19.2	65	1.3
B1	23.1	80	1.1
B2	23.8	80	1.0
B3	23.8	80	1.0
B4	22.2	80	1.1
B5	18.1	70	1.3
B6	14.2	40	1.7
F	8.8	25	2.5

c) Depth of cover: 300 m

The panel is found to be stable at a depth of 300 m and fulfills the design criteria. Fig. 6.6 shows the vertical stress and yielding profile of the panel at the mid-level of the pillars. The dark colors show higher stress values in the vertical stress profile, whereas the light colors show low-stress values. It has been observed from the vertical stress profile that the pillars near the goaf edge show high-stress values than the pillars far from the goaf edge. The yield profile shows that the pillars near the goaf edge have been highly yielded than the pillars far from the goaf edge. The pillars nearby goaf show a yielding of about 11 m from the side facing the goaf. The influence of the goaf has been observed up to one pillar from the goaf edge.

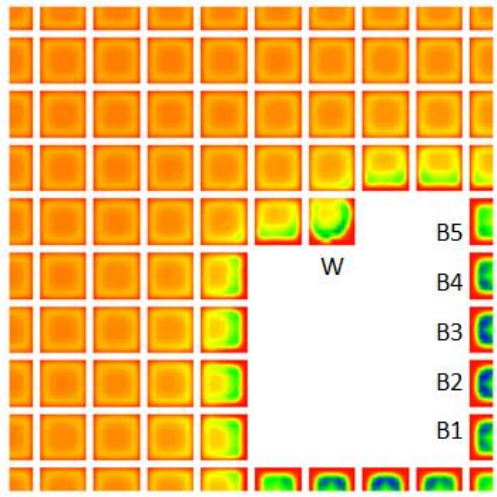

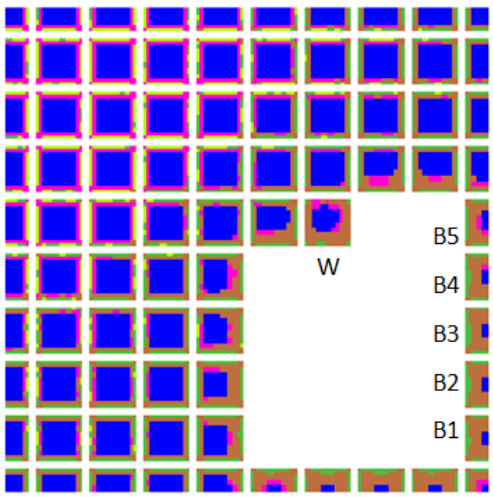

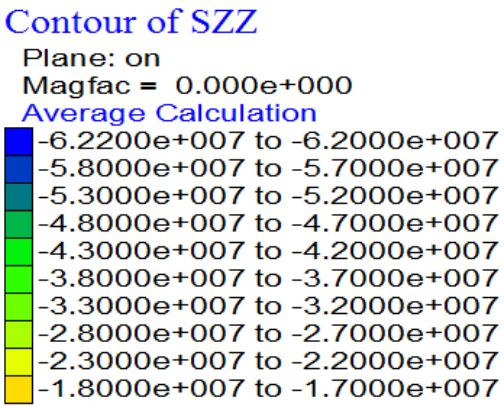

Vertical stress scale (stress in Pa)	Yielding state scale

Fig. 6.6 Vertical stress and yield profile of the panel with a pillar width of 45 m at a depth of 300 m

It has been observed from Fig. 6.6 that the barrier pillars have been yielded considerably with a small zone of the elastic core. The maximum stress value of about 62 MPa has been observed on the barrier pillars (B1 – B4). The barrier pillar ‘B2’ is the most critical barrier pillar in the panel, as seen from Fig. 6.6. The average vertical stress of the barrier pillar ‘B2’ has been observed as 25.8 MPa. The *FOS* of the critical barrier pillar ‘B2’ has been calculated as 1.0. It has further been observed that barrier pillar 'B6' has comparatively less stressed than the others due to the nearby intact pillars. The average vertical stress value on pillar 'B6' has been observed as 15.4

MPa. Table 6.6 shows the simulation results of the panel concerning the focused pillars. The yielding on the working pillar 'W' is asymmetric. More yielding has been observed on the sides of the pillar ‘W’ facing the goaf. On average, the working pillar 'W' has been yielded about 9 m from the sides, i.e., about 70%. The maximum vertical has been observed 8 m – 9 m inside the pillar (i.e., about 43 MPa).

Table 6.6 Simulation results of the panel with a pillar width of 45 m at a depth of 300 m

Pillar/Barrier No.	Average vertical stress (MPa)	Yield percentage (%)	FOS
W	19.8	70	1.3
B1	24.2	80	1.1
B2	25.8	80	1.0
B3	25.5	80	1.0
B4	24.2	80	1.1
B5	19.8	75	1.3
B6	15.4	45	1.7
F	10.0	20	2.5

Average vertical stress on the working pillars (i.e., 'W') has been computed as 19.8 MPa. The *FOS* of pillar ‘W’ has been calculated as 1.3. The pillars away from the goaf edge show a symmetrical stress distribution. The far-end pillar 'F' experiences a vertical stress value of about 10 MPa, equivalent to the stress at the development stage (10.0 MPa). The *FOS* of the far-end pillar ('F') has been calculated as 2.5.

d) Depth of cover: 330 m

The panel is stable at a depth of 330 m and fulfills the design criteria. Fig. 6.7 shows the vertical stress and yielding profile of the panel at the mid-level of the pillars. It has been observed from the vertical stress profile that the vertical stress on the pillars near to goaf edge is higher than the pillars far from the goaf edge. The yield profile shows that the pillar near the goaf edge has more yielded than the far end pillar. The yielding

of pillars near the goaf is about 12 m from the side facing the goaf. The influence of the goaf has been observed up to one pillar from the goaf edge.

The yielding on the working pillar 'W' is asymmetric. More yielding has been observed on the sides facing the goaf. On average, pillar 'W' has been yielded about 12 m from the sides, i.e., about 70%. The maximum stress has been observed 10 m – 12 m inside the working pillar, i.e., about 50 MPa. Average vertical stress on the working pillars (i.e., 'P') has been computed as 20.4 MPa. The *FOS* of the working pillar ‘W’ is 1.3.

It has been observed from Fig. 6.7 that the barrier pillars have been yielded considerably with a small zone of the elastic core. The maximum stress value of about 80 MPa has been observed on the barrier pillars (B1 – B4). The barrier pillar 'B2' is the most critical pillar of the panel. The average vertical stress on the critical barrier pillar ('B2') has been observed as 23.5 MPa. The FOS of the pillar ‘B2’ is 1.1. It has further been observed that barrier pillar 'B6' has comparatively less stressed than the others due to the intact pillars. The average vertical stress value on pillar 'B6' has been observed as 17.3 MPa. The panel satisfies the design criteria at a depth of 330 m, as shown in Fig. 6.7.

The pillars away from the goaf edge show a symmetrical stress distribution. The far-end pillar ‘F’ experiences a vertical stress value of about 11.1 MPa, equivalent to the stress at the development stage (11.0 MPa). The FOS of the far-end pillar ‘F’ has been calculated as 2.2. Table 6.7 shows the simulation results of the panel at a depth of 330 m.

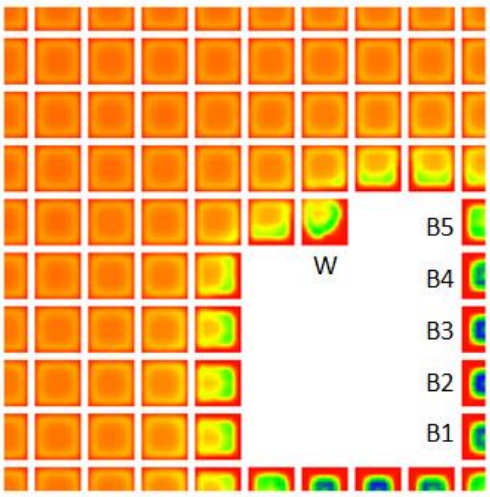

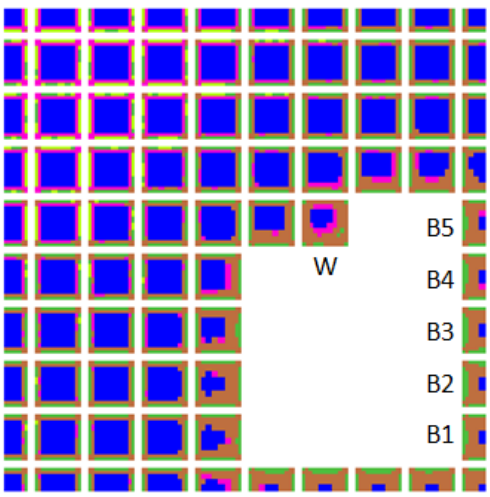

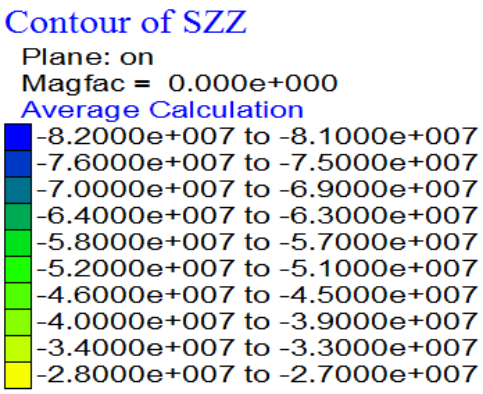

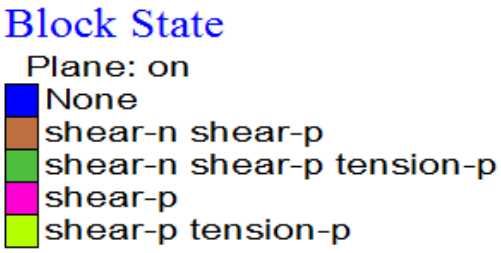

Vertical stress scale (stress in Pa)	Yielding state scale

Fig. 6.7 Vertical stress and yield profile of the panel with a pillar width of 45 m at a depth of 330 m

Table 6.7 Simulation results of the panel with a pillar width of 45 m at a depth of 330 m

Pillar/Barrier No.	Average vertical stress (MPa)	Yield percentage (%)	FOS
W	20.4	75	1.3
B1	22.5	80	1.2
B2	23.5	80	1.1
B3	23.2	80	1.1
B4	21.6	80	1.2
B5	21.8	80	1.2
B6	17.3	50	1.5
F	11.1	20	2.2

e) Depth of cover: 360 m

The simulation results show that the panel is unstable at a depth of 360 m. The barrier panels surrounded by the goaf from both sides failed at a depth of 360 m, resulting in extreme loading conditions near the working area. The vertical stress and yielding profile of the panel at a depth of 360 m have been provided in Appendix – B3.

6.2.4. Simulation results for pillar width of 48 m

The panel with a pillar width of 48 m has been simulated for a depth range of 360 m – 450 m. The simulation results have been obtained in terms of vertical stress profile and yield profile. The dark color (blue) in the vertical stress profile shows higher stress values, whereas the light color (like yellow) shows lower stress values in the vertical stress profile. The average vertical stress on the focused pillars has been determined through *the FISH* function of *FLAC*^{3D}. The pillar strength has been determined separately using the numerical technique (i.e., 33.5 MPa). The FOS of the focused pillars has been determined for all the cases. The stable cases of the panel satisfying the design criteria have been discussed in this section.

a) Depth of cover: 360 m

The panel is found to be stable at a depth of 360 m and fulfills the design criteria. Fig. 6.8 shows the vertical stress and yielding profile of the panel at the mid-level of the pillars. It has been observed from the vertical stress profile that the pillars near to goaf edge show high yielding than the pillars far from the goaf edge. The yield profile shows that the pillar near the goaf edge has more yielded than the far end pillar. The pillars nearby goaf show a yielding of about 18 m from the side facing the goaf. The influence of the goaf has been observed up to one pillar from the goaf edge.

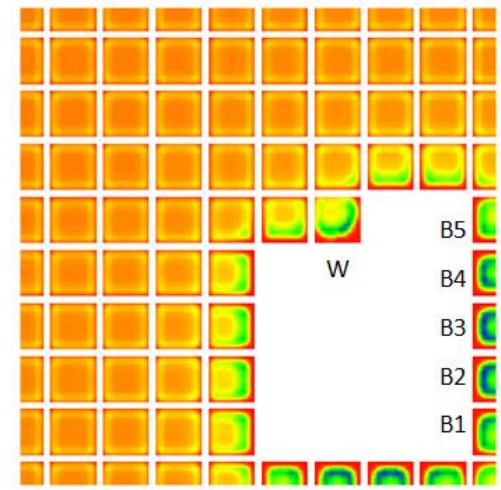

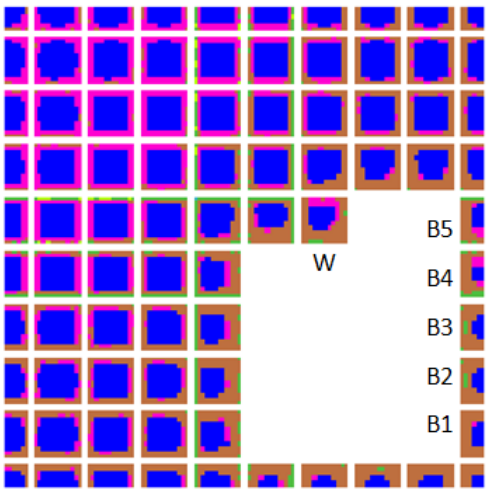

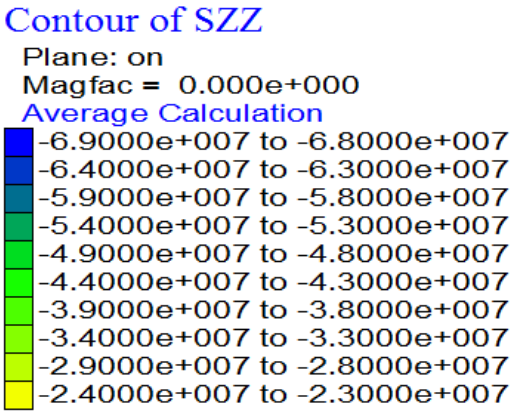

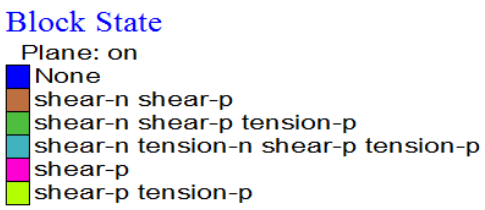

Vertical stress scale (stress in Pa)	Yielding state scale

Fig. 6.8 Vertical stress and yield profile of the panel with a pillar width of 48 m at a depth of 360 m

It has been observed from Fig. 6.8 that the barrier pillars have been yielded considerably with a small zone of the elastic core. The maximum stress value of about 65 MPa has been observed on the barrier pillars (B2 – B4). The pillar 'B2' is the most critical pillar of the panel. The average vertical stress on pillar ‘B2’ has been observed as 29.5 MPa. The *FOS* of the critical barrier pillar ‘B2’ has been calculated as 1.1. It has further been observed that barrier pillar 'B6' has comparatively less stressed than the others due to the intact pillars. The average vertical stress value on pillar 'B6' has been observed as 17.7 MPa. The yielding on the working pillar 'W' is asymmetric.

More yielding has been observed on the sides facing the goaf. On average, pillar 'W' has been yielded about 15.0 m from the sides, i.e., about 65%. The maximum stress has been observed 12 m – 13 m inside the pillar, i.e., about 45 MPa. Average vertical stress on the working pillars (i.e., 'W') has been computed as 22.8 MPa. The *FOS* of pillar 'W' has been calculated as 1.5. The pillars away from the goaf edge show a symmetrical stress distribution. The far-end pillar ('F') experiences a vertical stress value of about 11.9 MPa, equivalent to the stress at the development stage (11.8 MPa). The *FOS* of the far-end pillar ('F') has been calculated as 2.5. Table 6.8 shows the simulation results of the panel concerning the focused pillars.

Table 6.8 Simulation results of the panel with a pillar width of 48 m at a depth of 360 m

Pillar/Barrier No.	**Average vertical stress (MPa)**	**Yield percentage (%)**	**FOS**
W	22.8	65	1.5
B1	27.4	70	1.2
B2	29.2	75	1.1
B3	29.5	75	1.1
B4	27.7	80	1.2
B5	23.5	70	1.4
B6	17.7	45	1.9
F	11.9	25	2.5

b) Depth of cover: 390 m

The panel is stable at a depth of 390 m and fulfills the design criteria. Fig. 6.9 shows the vertical stress and yielding profile of the panel at the mid-level of the pillars. It has been observed that the vertical stress on the pillars near to goaf edge is higher than the pillars far from the goaf edge. The pillar near the goaf shows higher yielding than the far end pillar (i.e., about 23 m from the side facing the goaf). The influence of the goaf has been observed up to one pillar from the goaf edge. The yielding on the

working pillar 'W' is asymmetric. More yielding has been observed on the sides facing the goaf. On average, pillar 'W' has been yielded about 25.0 m from the sides, i.e., about 75%. The maximum stress has been observed 10 m – 12 m inside the pillar, i.e., about 55 MPa. Average vertical stress on the working pillars (i.e., 'W') has been computed as 21.5 MPa. The FOS of the working pillar ‘W’ has been calculated as 1.6.

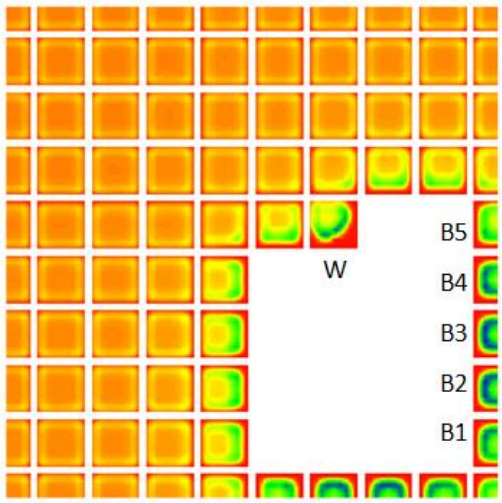

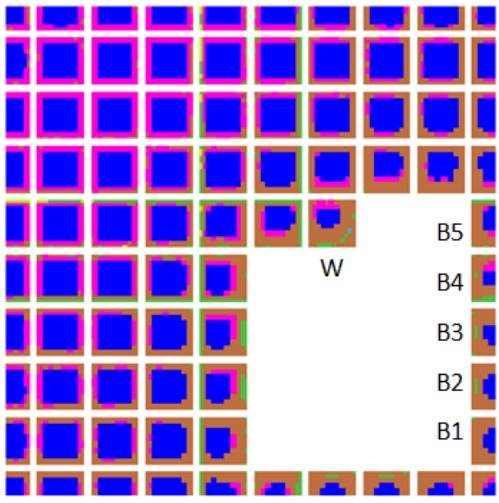

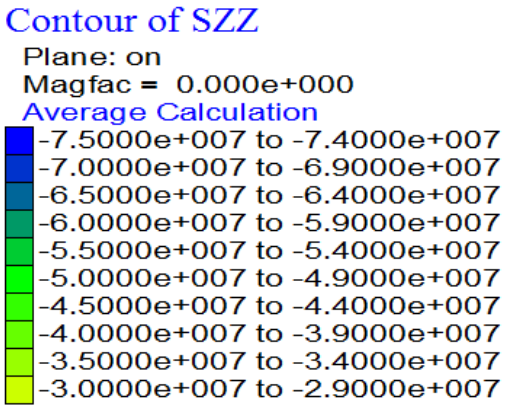

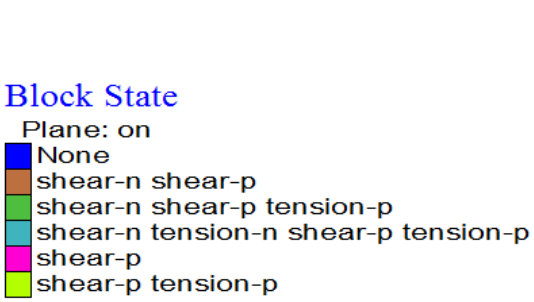

Vertical stress scale (stress in Pa)	Yielding state scale

Fig. 6.9 Vertical stress and yield profile of the panel with a pillar width of 48 m at a depth of 390 m

It has been observed from Fig. 6.9 that the barrier pillars have been yielded considerably with a small zone of the elastic core. The maximum stress value of about 75 MPa has been observed on the barrier pillars (B2 – B4). The barrier pillar 'B2' is

the most critical pillar of the panel, with average vertical stress of about 31.5 MPa. The *FOS* of the critical barrier pillar ‘B2’ has been computed as 1.1.

It has further been observed that barrier pillar 'B6' has comparatively less stressed than the others due to the nearby intact pillars. The average vertical stress value on pillar 'B6' has been observed as 19 MPa. The pillars away from the goaf edge show a symmetrical stress distribution. The pillar 'F,' which is at the far-end from the goaf, shows a vertical stress value of about 13.1 MPa, equivalent to the stress at the development stage (12.7 MPa). The *FOS* of the far-end pillar (‘F’) has been calculated as 2.3. Table 6.9 shows the simulation results of the panel concerning the focused pillars.

Table 6.9 Simulation results of the panel with a pillar width of 48 m at a depth of 390 m

Pillar/Barrier No.	**Average vertical stress (MPa)**	**Yield percentage (%)**	**FOS**
W	21.5	75	1.6
B1	28.7	70	1.2
B2	31.4	70	1.1
B3	31.5	75	1.1
B4	30.1	80	1.1
B5	25.5	70	1.3
B6	19.0	50	1.8
F	13.1	25	2.3

c) Depth of cover: 420 m

The panel is stable at a depth of 420 m and fulfills the design criteria. Fig. 6.10 shows the vertical stress and yielding profile of the panel at the mid-level of the pillars. It has been observed from the vertical stress profile that the pillars near to goaf edge show higher vertical stress than the pillars far from the goaf edge. The yield profile shows that the pillar near the goaf edge has more yielded than the far end pillar. The pillar

near the goaf shows a yielding of about 20 m from the side facing the goaf. The influence of the goaf has been observed up to one pillar from the goaf edge.

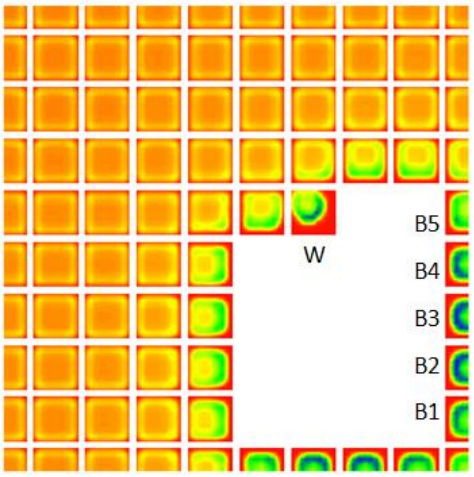

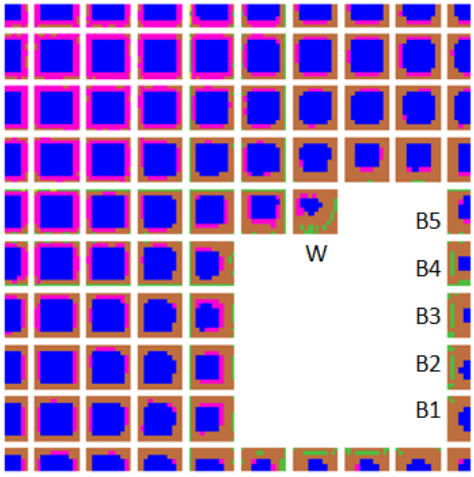

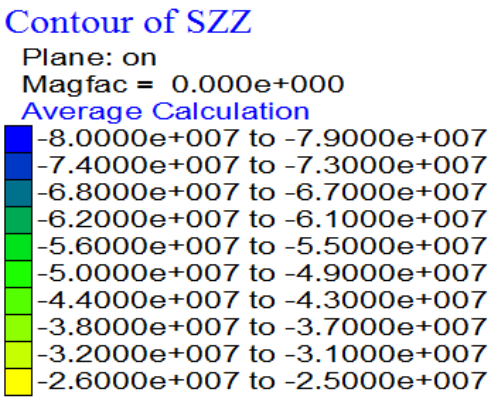

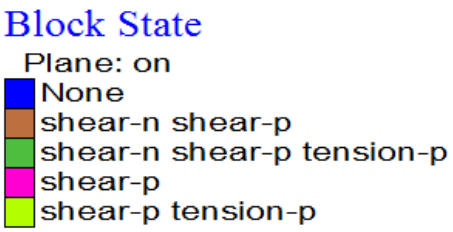

Vertical stress scale (stress in Pa)	Yielding state scale

Fig. 6.10 Vertical stress and yield profile of the panel with a pillar width of 48 m at a depth of 420 m

It has been observed from Fig. 6.10 that the barrier pillars have been yielded considerably with a small zone of the elastic core. The barrier pillars (B2 – B4) show a maximum stress value of about 80 MPa. The barrier pillar ‘B2’ is observed to be the most critical pillar in the panel. The average vertical stress on pillar ‘B2’ has been observed as 33.4 MPa. The *FOS* of the critical barrier pillar ‘B2’ has been calculated as 1.0. It has further been observed that barrier pillar 'B6' has comparatively less

stressed than the others due to the nearby intact pillars. The average vertical stress value on pillar 'B6' has been observed as 20.2 MPa.

The yield profile shows that the yielding of working pillar ‘W’ is asymmetric. More yielding has been observed on the sides facing the goaf. On average, pillar 'W' has been yielded about 25.0 m from the sides, i.e., about 80%. The maximum stress has been observed 11 m – 12 m inside the pillar, i.e., about 60 MPa. Table 6.10 shows the simulation results of the panel at a depth of 420 m.

Table 6.10 Simulation results of the panel with a pillar width of 48 m at a depth of 420 m

Pillar/Barrier No.	Average vertical stress (MPa)	Yield percentage (%)	FOS
W	20.1	80	1.7
B1	30.7	70	1.1
B2	33.4	75	1.0
B3	33.0	80	1.0
B4	31.2	75	1.1
B5	27.3	70	1.2
B6	20.2	55	1.7
F	14.2	25	2.1

Average vertical stress on the working pillars (i.e., 'W') has been computed as 20.1 MPa. The *FOS* of pillar ‘W’ has been calculated as 1.7. The pillars away from the goaf edge show a symmetrical stress distribution. The pillar 'F,' which is far from the goaf edge, experiences a vertical stress value of about 14.2 MPa, equivalent to the stress at the development stage (13.7 MPa). The *FOS* of the far-end pillar (‘F’) has been calculated as 2.1.

d) Depth of cover: 450 m

The simulation results show unstable mining conditions in the panel at a depth of 450 m. The working pillar ultimately failed at a depth of 450 m, which results in extreme

loading conditions on the nearby intact pillars. The vertical stress and yielding profile of the panel at a depth of 450 have been provided in Appendix – B4.

6.2.5. Analysis for panel design

The pillars are the key elements of a bord and pillar panel. The stability of the pillars/barriers plays an essential role in providing safe mining conditions. The pillars nearby goaf show high vertical stress during the depillaring operation. The working and the barrier pillars (which are surrounded by the goaf from both sides) are the most critical pillars of the panel. The stability of these focused pillars (working/barrier) is the prime necessity for a successful depillaring operation, as the extraction of an unstable pillar leads to raising the strata issues in the working area. Also, the failure of the barrier pillars results in extreme loading conditions in the working area. The focused pillars (working/barrier) show maximum vertical stress value at a depillaring stage in which the advancement length is equivalent to the panel width. The stability of the focused pillars (working/barrier) has been accessed in the study using numerical techniques. Panels of four different pillar sizes (i.e., having pillar width of 26 m, 35 m, 45 m, and 48 m) have been simulated at a critical depillaring stage for different depths ranging from 90 m to 450 m with an interval of 30 m. The stable cases of the panels satisfying the design criteria have been chosen for the analysis. The change in the stress dynamics of the pillars during development and depillaring has been accessed in the study with different pillar widths and depths of cover. The average vertical stress on the pillars during development has been determined using tributary area theory. The average vertical stress on the focused pillars (working/barrier) during depillaring has been determined using the *FISH* function of *FLAC*^{3D}.

The simulation result shows that the average vertical stress on the pillars increases with the increase in depth of cover and pillar width. Fig. 6.11 shows the graphical representation of the average vertical stress on the focused pillars (working/barrier) at different pillar widths and depths. The blue color in Fig. 6.11 shows the average vertical stress on the barrier pillar, whereas the green color shows the average vertical stress on the working pillar during depillaring. The red color in Fig. 6.11 shows the average vertical stress on the pillars during development. A linear increment in the average vertical stress has been observed on the focused pillars (working/barrier) with increased depths. The magnitude of increment is slightly higher in the barrier pillar than the working pillar, as seen in Fig. 6.11.

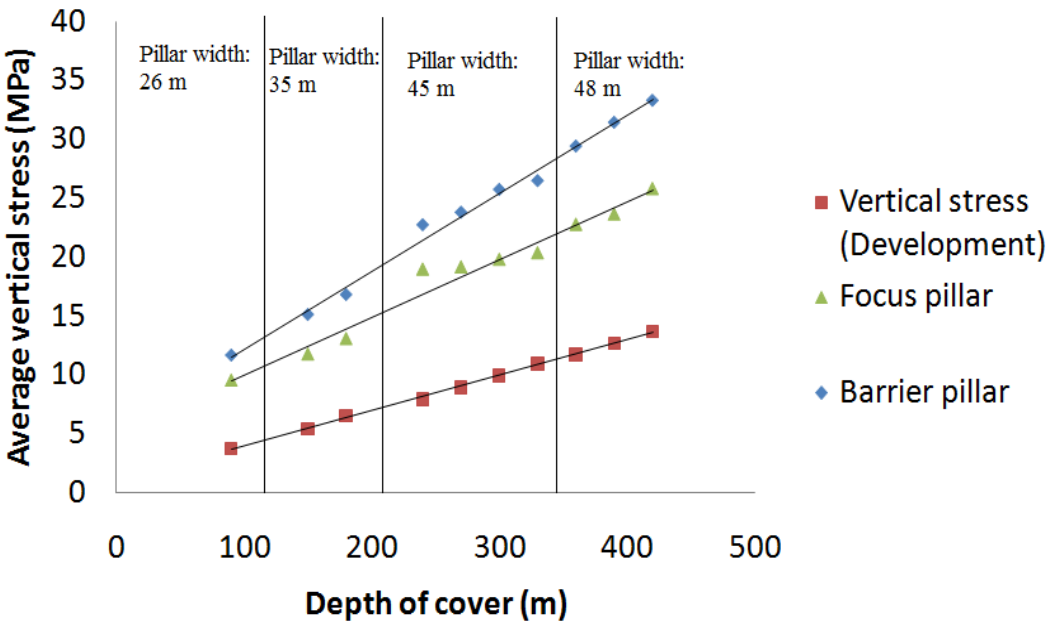

Fig. 6.11 Average vertical stress on the selected pillars at different depth of cover

The change in the average vertical stress on the focused pillars (working/barrier) during depillaring for different pillar widths has been observed in the study, as shown in Fig. 6.12. It has been observed from Fig. 6.12 that the magnitude of the average vertical stress in the barrier pillar is higher than the working pillar. The blue and green

color in Fig. 6.12 shows the average vertical stress on the barrier and working pillar, respectively. The average vertical stress on the pillars during development has been presented in the graph (fig. 6.12) with red color. It has been observed from Fig. 6.12 that the average vertical stress on the pillars shows an exponential relationship with the pillar width.

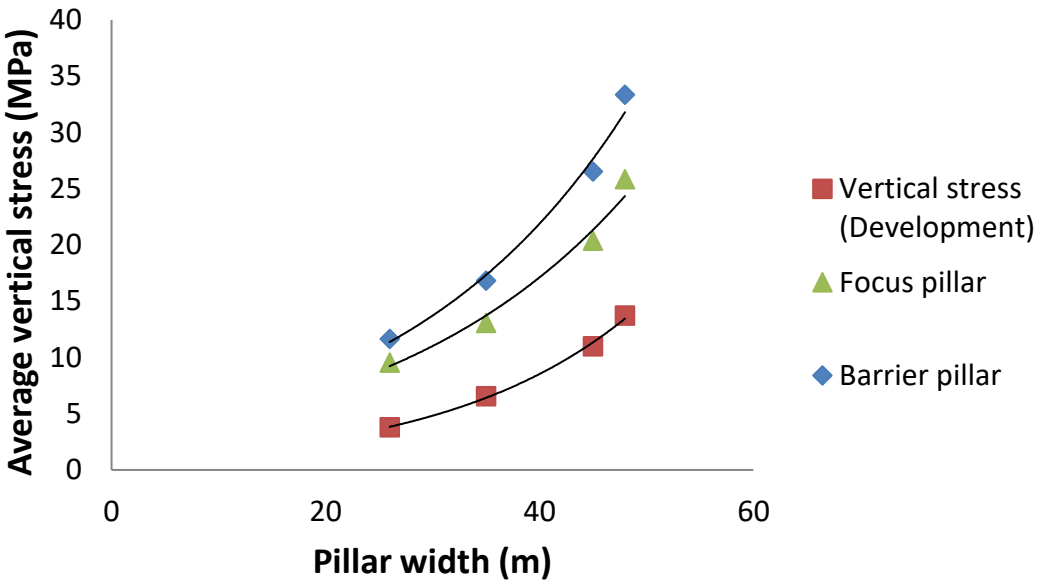

Fig. 6.12 Average vertical stress on the selected pillar

The simulation results of the stable cases of the panels concerning the focused pillars (working/barrier) have been arranged in a tabular format for the analysis, as shown in Table 6.11. The analysis shows that the panel with a pillar width of 26 m is stable up to the depth of 90 m, and the critical depth of cover of pillar width of 35 m, 45 m, and 48 m has been obtained as 180 m, 330 m, and 420 m, respectively.

Table 6.11 Average vertical stress on the pillars during development and depillaring

Pillar width (m)	Depth of cover (m)	Vertical stress (Development) (MPa)	Vertical stress (Depillaring) (MPa)	
			Working pillar	Barrier pillar
26	90	3.8	9.55	11.56
35	150	5.46	11.77	15.11
35	180	6.55	13.08	16.81
45	240	7.99	18.99	22.76
45	270	8.99	19.18	23.83
45	300	9.99	19.81	25.77
45	330	10.98	20.38	23.48
48	360	11.76	22.8	29.47
48	390	12.73	23.67	30.5
48	420	13.71	25.84	31.1

The ratio of the average vertical stress on the pillar during depillaring and development has been calculated in the analysis and is termed as '*Stress ratio (SR)*' (Eq. 6.1).

$$Stress\ ratio = \frac{Average\ vertical\ stress\ during\ depillaring}{Average\ vertical\ stress\ during\ development} \quad (6.1)$$

The *SR* has been calculated for each stable case, as shown in Table 6.12. The analysis shows that the *SR* for both the working and barrier pillar decreases with an increase in depth. The *SR* for the working pillar varies from 1.9 - 2.5 in between the depth range of 90 m – 450 m, whereas in the same depth range, the *SR* for the barrier pillar ranges from 2.4 – 3.0.

A wide range of *SR* has been observed for different cases (i.e., panel having different pillar widths and depths) as seen from Table 6.12. The trend of the *SR* is not uniform with the depth of cover and pillar width. Thus, an attempt has been made to co-relate the *SR* with the *FOS* of the pillar during development. The *FOS* of the pillars during development has been calculated for a different combination of pillar width and depth of cover, as shown in Table 6.12.

Table 6.12 Stress ratio of the focused pillars during depillaring

Depth of cover (m)	Pillar width (m)	FOS (Development)	Stress ratio (SR)	
			Working pillar	Barrier pillar
90	26	3.3	2.5	3.0
150	35	3.1	2.2	2.8
180	35	2.6	2.0	2.6
240	45	3.5	2.4	2.8
270	45	3.1	2.1	2.7
300	45	2.8	2.0	2.6
330	45	2.6	1.9	2.4
360	48	2.6	1.9	2.5
390	48	2.4	1.9	2.5
420	48	2.3	1.9	2.4

The graphical representation of the *SR* of the pillars with its *FOS* during development has been shown in Fig. 6.13. A linear relationship has been observed during the analysis between the *SR* of the focused pillars (working/barrier) and their *FOS* during development. The analysis shows that the pillars with high *FOS* during development have a more elastic limit and show more *SR* value.

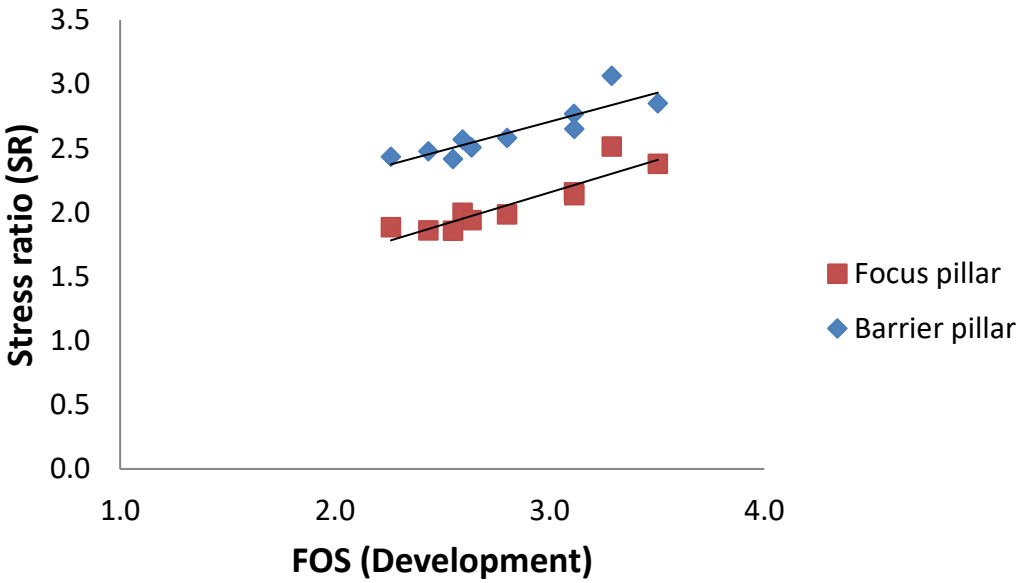

Fig. 6.13 Stress ratio (*SR*) for the pillar with different *FOS* during development

A linear relationship has been observed from the analysis between the *SR* and the *FOS* of the pillars during development. The *SR* for the working and barrier pillar can be determined using Eq. 6.2 and 6.3, respectively.

$$SR_W = 0.5\ x\ FOS_{Development} + 0.6 \quad (6.2)$$

$$SR_B = 0.45\ x\ FOS_{Development} + 1.3 \quad (6.3)$$

6.2.6. Guidelines for panel design

The success of the mechanized depillaring operation mainly depends on the design of the intact pillars and remnant pillars (ribs/snook). The working and the barrier pillars (which are surrounded by goaf from both sides) are the critical pillars of a depillaring panel. The stability of the focused pillars (working/barrier) governs the strata issues and provides safe mining conditions. The *FOS* approach has been used in the study to design the pillars for mechanized depillaring. The *FOS* of the working pillar should not be less than 1.3 (preferably above 1.5), and the *FOS* of the barrier pillar should be above 1.0 for a safe depillaring operation. An expression has been derived to determine the '*Stress ratio (SR)*' of a pillar based on its *FOS* during development. The ratio of the average vertical stress on the pillar during depillaring and development is termed as *SR*. The average vertical stress on the pillar and its *FOS* during depillaring can be determined easily after knowing its *SR*. One can access the stability of the mechanized depillaring panel by obtaining the *FOS* of the pillars during depillaring. The pillar width needs to be adjusted when the *FOS* of the working and barrier pillars during depillaring does not meet the design criteria. An illustration has been provided to determine the *FOS* of the pillar during depillaring.

Illustration 6.1 Panel design for mechanized depillaring

The steps to be followed while designing the mechanized depillaring panel are:

Step 1: Select the depth of cover (Let the depth be 330 m)

Step 2: Choose a pillar width (Let the pillar width be 45 m)

Step 3: Determine the average vertical stress on the pillar during development using tributary area theory:

$$Average\ vertical\ stress_{Development} =$$

$$0.025\ x\ (Depth) x\ \frac{(Pillar\ width)^2}{(Pillar\ width - Gallery\ width)^2}$$

For the present case:

$$Average\ vertical\ stress_{Development} = 0.025\ x\ (330) x\ \frac{(45)^2}{(45-6)^2}$$

$$Average\ vertical\ stress_{Development} = 10.98\ MPa$$

Step 4: Determine the strength of the pillar (Empirically or numerically)

For the present case, the pillar strength has been determined numerically and found to be 28 MPa.

Step 5: Determine the *FOS* of the pillar during development

$$FOS_{Development} = \frac{Strength}{Stress_{Development}}$$

For the present case, the FOS of the pillar was:

$$FOS_{Development} = \frac{28}{10.98}$$

$$FOS_{Development} = 2.5$$

Step 6: Determine the '*Stress ratio*' for the selected pillar using Eq. 6.1

$$Stress\ ratio = 0.55\ x\ \left(FOS_{development}\right) +\ 0.5$$

$$Stress\ ratio = 0.55\ x\ (2.5) +\ 0.5$$

$$Stress\ ratio = 1.87$$

Step 7: Determine the average vertical stress on the pillar during depillaring

$$Vertical\ stress_{Depillaring} = Stress\ ratio x\ Vertical\ stress_{Development}$$

$$Vertical\ stress_{Depillaring} = 1.87\ x\ 10.98$$

$$Vertical\ stress_{Depillaring} = 20.53\ MPa$$

Step 8: Determine the *FOS* of the pillar during depillaring

$$FOS_{Depillaring} = \frac{Strength}{Stress_{Depillaring}}$$

$$FOS_{Depillaring} = \frac{28}{20.53}$$

$$FOS_{Depillaring} = 1.36$$

Step 9: If the *FOS* of the pillar during depillaring is equal or more than 1.3, the design of the pillar was considered to be optimum; else, increase the width of the pillar to achieve safe depillaring operation.

For the present case, the $FOS_{depillaring}$ has been calculated as 1.36, which satisfies the design criteria. Hence, the chosen pillar width is optimum for a mechanized depillaring panel.

Note: In the case of an already developed panel, the pillar size cannot be increased. It has been suggested in the study to leave an extra row of barrier pillars (towards the goaf side) if the $FOS_{depillaring}$ was found to be less than 1.3.

One can design the *CM* depillaring panel using the above-mentioned guidelines. Based on the design guidelines, a nomograph has been developed in the study to determine the optimum width of the pillar for a mechanized depillaring panel (considering *UCS* of coal as 40 MPa) under different depths of cover and extraction height, as shown in Table 6.13.

Table 6.13 Nomograph showing the optimum width of the pillar for a mechanized depillaring panel

Depth of cover (m)	**Extraction height (m)**					
	3	3.5	4	4.5	5	5.5
	Optimum pillar width for CM working (m)					
100	18	20	20	22	23	24
150	25	29	30	32	34	36
200	29	35	35	38	41	44
250	33	39	39	44	46	49
300	35	43	43	47	51	54
350	38	46	46	50	54	58
400	40	49	49	53	58	62
450	41	51	51	56	60	65

6.3.Remnant pillar design

The design of the remnant pillars (ribs/snook) plays an important role in maintaining the local stability of the panel during the depillaring operation. The immediate strata separate from the main strata forming a cantilever during the depillaring operation and impose its load on the remnant pillars. The role of a remnant pillar is to provide temporary support to the immediate strata and maintain stable mining conditions in the working area. Over-sized remnant pillars generally delay the caving process, whereas an under-sized remnant pillars may raise an overriding situation in the

working area. An optimum remnant pillar design is considered to be the one in which the residual strength of the remnant pillar is sufficient enough to bear the load of the overhang (immediate strata) until depillaring advances to a safe distance.

The remnant pillar undergoes residual phase during the depillaring operation due to overhang load and smaller size of ribs/snook. Numerical techniques have been used in the study to assess the stability of the remnant pillars during the depillaring operation. The thickness and density of the immediate strata have been taken as 4.0 m and 2.5 g/cm^2, considering field investigations. The area of the overhang has been considered to be one pillar size. Numerical models for the depillaring panels having pillar widths of 26 m, 35 m, 45 m, and 48 m have been prepared in the study. The height of the pillar has been considered as 4.5 m. The models have been simulated at a critical depillaring stage at which the advancement length is equivalent to the panel width. The maximum depth of cover up to which the panel is stable, as determined through the panel design exercise (Section 6.2), has been chosen for designing the remnant pillars for each selected pillars, i.e., having a pillar width of 26 m, 35 m, 45 m, and 48 m,. The working pillar has been discretized in the model such that the splitting and slicing operation can be performed at different stages until complete extraction of the working pillar (i.e., pillar ‘W’). The previously extracted pillar (i.e., pillar 'P') has also been considered in a similar manner forming ribs/snooks.

The term '*Strength Factor (SF)*' has been coined in the study to assess the stability of the remnant pillar. The *SF* is the ratio of the residual strength of the remnant pillars and the weight of the overhang. The optimum remnant pillar design is considered to be the one in which the constructed such that the *SF* of remnant pillar ‘P’ (previously extracted pillar) is less than 1.0 and *SF* of remnant pillar 'W' (working pillar) is more than 1.0 at a depillaring stage where the last slice has been taken out from the working

pillar ('W'). The optimum remnant pillar design has been obtained in the study by varying the size of the snook. Three different snook sizes, i.e., having a resultant width of 4.5 m, 5.5 m, and 6.5 m, have been considered for each case of pillars.

The optimum design of the remnant pillars for each selected pillars (i.e., having pillar width of 26 m, 35 m, 45 m, and 48 m), which fulfills the design criteria, has been discussed in this section. The simulation results were obtained in terms of vertical stress profile and yield profile of the pillars/remnants at the mid-level. The simulation results have been presented such that the plan view of the complete panel has been shown for the 1st depillaring stage, and a zoomed view of the focused remnant pillars (i.e., remnant pillar 'W' and remnant pillar 'P') has been provided for the rest of the depillaring stages. The other cases of the remnant pillars which do not satisfy the design criteria have been provided in the Appendix - C.

6.3.1. Simulation results for pillar width of 26 m

The panel has a pillar width of 26 m has been simulated at a depth of 90 m, adopting the fish-bone pattern of extraction. The working pillar (‘W’), previously extracted pillar (‘P’), and the immediate next pillar (‘N’) have been constructed in such a manner that slices can be taken out from the pillar at different depillaring stages. The model has been simulated for four different depillaring stages (i.e., *'Stage I'* through *'Stage IV'*). The simulation results were obtained in terms of vertical stress and yield profile. The dark color (blue) in the vertical stress profile depicts high vertical stress values, whereas the light color (yellow, orange) depicts lower stress values. The load-bearing capacity of the remnant pillars has been determined through the *FISH* function of *FLAC*^{3D}. The ‘*Strength factor (SF)’* of the focused pillar/remnants (i.e., ‘W’ and ‘P’) has been determined for all the cases of the remnant pillars (i.e., having

snook width of 4.5 m, 5.5 m, and 6.5 m). The simulation results of the optimum remnant pillar design satisfying the design criteria have been discussed in this section. The rest cases of the remnant pillar which does not satisfy the design criteria have been provided in the Appendix – C1.

Fig. 6.14 shows the vertical stress and yielding profile of the panel during *'Stage I,*' where the first slice has been taken out from the pillar. The working pillar shows yielding of about 70% during *'Stage I'* and shows maximum stress of about 23 MPa, as seen from Fig. 6.14b. The average vertical stress on the working pillar/remnant 'W' has been obtained as 8.39 MPa. The previously extracted pillar ('P') yields entirely at this stage and shows average vertical stress of about 1.08 MPa. The immediate next pillar ('N') yields about 20% at '*Stage I*' and shows average vertical stress of about 7.45 MPa.

The simulation results of the next depillaring stages (i.e., *'Stage II'* through *'Stage IV'*) have been shown in Fig. 6.15. At *'Stage II,'* the maximum stress of about 23 MPa has been observed on the intact portion of the working pillar ('W'), as seen by the blue color in the vertical stress profile (fig. 6.15a). The working pillar ('W') yields about 95% at this stage and shows average vertical stress of about 6.27 MPa. The average vertical stress on pillar 'P' reduces to 0.48 MPa. A slight increment in the stress values has been observed in the immediate next pillar ('N'). The average vertical stress on pillar 'N' during *'Stage II'* has been observed as 8.13 MPa, though a negligible change has been observed in the yield percentage at this stage.

At *'Stage III,'* the working pillar yields entirely, and a significant reduction in the vertical stress value has been observed in pillar 'W' as seen from Fig. 6.15b. The average vertical stress on pillar 'W' during '*Stage III*' has been observed as 1.66 MPa.

The immediate next pillar ('N') yields about 70% at this stage and shows an average vertical is about 8.22 MPa. The average vertical stress on pillar 'P' during '*Stage III*' has been observed as 0.48 MPa.

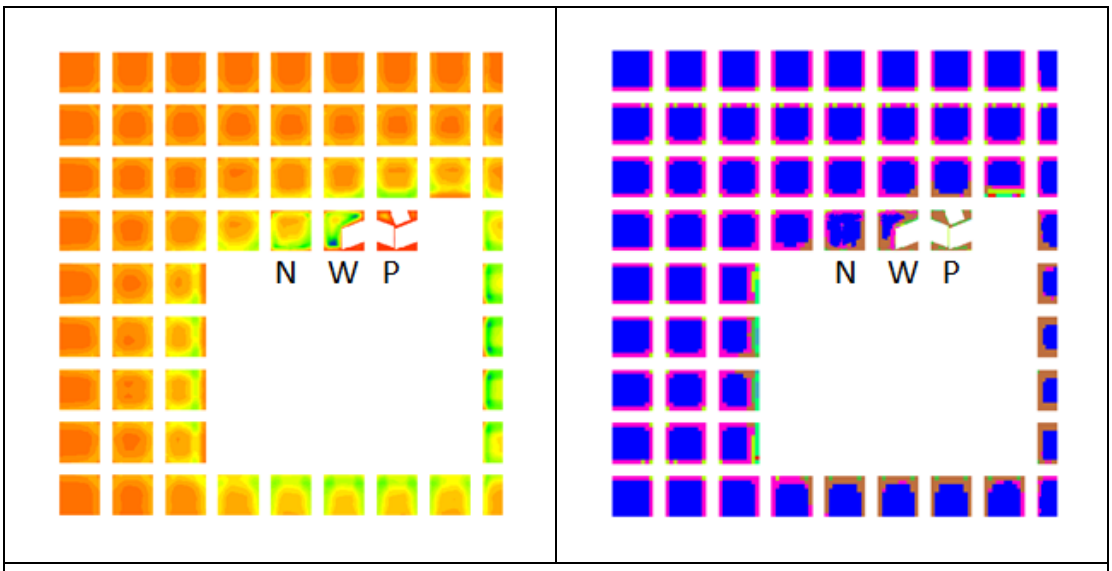

a. Stage I (Plan view)

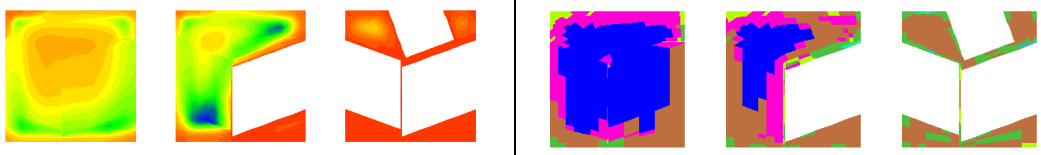

b. Stage I (Zoomed view)

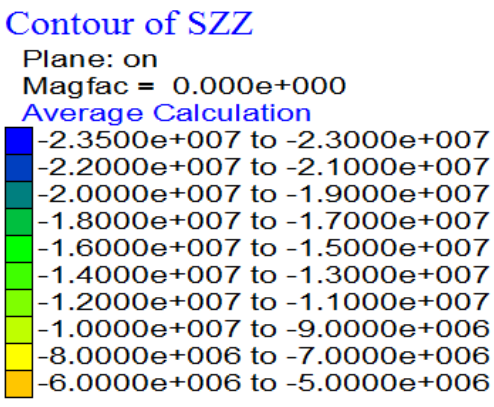

Vertical stress scale (stress in Pa)

Yielding state scale

Fig. 6.14 Vertical stress and yield profile of the panel with a pillar width of 26 m and snook width of 4.5 m at a depth of 90 m during 'Stage I'

At '*Stage IV*,' the average vertical stress on the working pillar ('W') reduces to 0.63 MPa. The previously extracted pillar ('P') shows average vertical stress of about 0.32 MPa at this stage. The vertical stress and yield profile of the immediate next pillar ('N') during *'Stage IV'* is similar to the previous stage, as seen from Fig. 6.15c. The average vertical stress on pillar 'N' at this stage has been observed as 8.23 MPa.

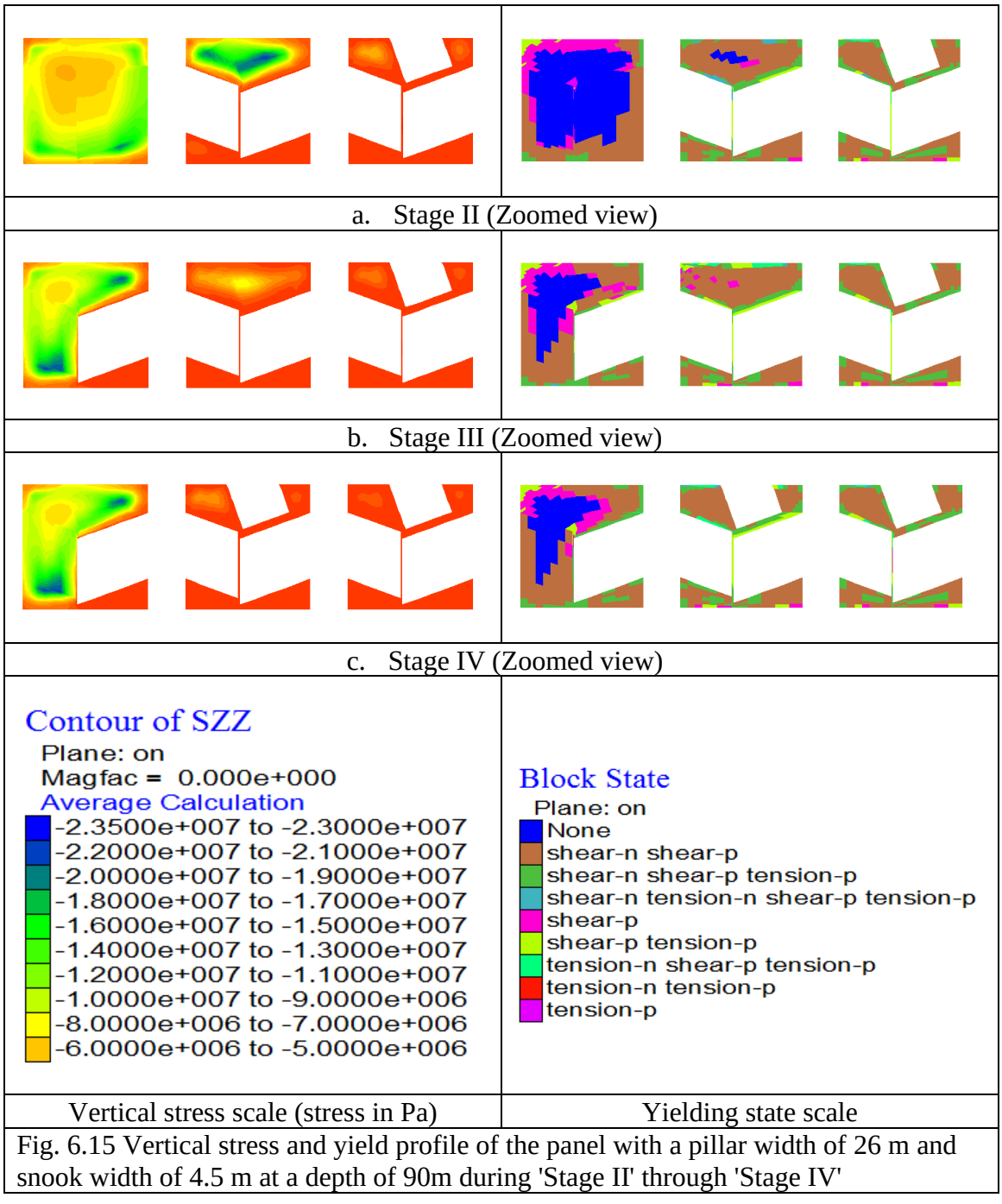

Fig. 6.15 Vertical stress and yield profile of the panel with a pillar width of 26 m and snook width of 4.5 m at a depth of 90m during 'Stage II' through 'Stage IV'

The '*Strength Factor (SF)'* of the concerned pillars/remnants, i.e., working pillar ('W'), the previously extracted pillar ('P'), and the immediate next pillar ('N'), has been calculated at each stage of depillaring. The weight of the overhang in this scenario has been calculated as 6,760 T (Eq. 3.2). Table 6.14 shows the simulation results of the panel at four different depillaring stages. The simulation shows that the working pillar ('W') yields completely during *'Stage III'* and shows an *SF* value of about 4.5. The *SF* of the working pillar 'W' and the previously extracted pillar 'P' during the last stage (*'Stage IV'*) has been calculated as 1.2 and 0.6.

Table 6.14 Simulation results of the remnant pillars for a pillar width of 26 and snook width of 4.5 m at a depth of 90 m

Stage	**Previously extracted pillar ('P')**			**Working pillar ('W')**			**Next pillar ('N')**		
	Average vertical stress (MPa)	**Yield (%)**	**SF**	**Average vertical stress (MPa)**	**Yield (%)**	**SF**	**Average vertical stress (MPa)**	**Yield (%)**	**SF**
1	1.08	100	2.2	8.39	70	-	7.45	20	-
2	0.82	100	1.6	6.27	95	-	8.13	20	-
3	0.48	100	0.9	1.66	100	4.5	8.22	70	-
4	0.32	100	0.6	0.65	100	1.3	8.23	70	-

'-' shows that an intact core is present in the pillar/remnant

6.3.2. Simulation results for pillar width of 35 m

The pillar width of 35 m has been simulated at a depth of 180 m adopting a split and fender extraction pattern. The working pillar ('W'), and the previously extracted pillar ('P'), have been constructed so that splitting and slicing operations can be performed at different depillaring stages. The model has been simulated for six different depillaring stages (*'Stage 0*' through *'Stage V*'). The simulation results were obtained in terms of vertical stress and yield profile. The dark color (blue) in the vertical stress profile depicts high vertical stress values, whereas the light color (yellow, orange)

depicts lower stress values. The load-bearing capacity of the remnant pillars has been determined through the *FISH* function of *FLAC*^{3D}. The '*Strength factor (SF)'* of the concerned pillar/remnants (i.e., 'W' and 'P') has been determined for all the cases of the remnant pillars (i.e., having snook width of 4.5 m, 5.5 m, and 6.5 m). The simulation results of the optimum remnant pillar design satisfying the design criteria have been discussed in this section. The rest cases of the remnant pillars which does not satisfy the design criteria have been provided in the Appendix – C2.

Fig. 6.16 shows the vertical stress and yielding profile of the pillars during *'Stage 0,'* i.e., before splitting the working pillar ('W'). The vertical stress and yield profile reveal that goaf's influence is up to one row of pillars, as seen from Fig. 6.16a. The maximum stress of about 39 MPa has been observed in the working pillar ('W') as indicated by blue color (fig. 6.16). The working pillar 'W' yields about 70% at this stage and shows average vertical stress of about 12.54 MPa. The zoomed view of the focused pillars ('W' and 'P') has been shown in Fig. 6.16b. The previously extracted pillar ('P') yields entirely during *'Stage 0'* and shows the average vertical stress of about 0.66 MPa.

Fig. 6.17 shows vertical stress and yield profile of the focused pillar (i.e., 'W' and 'P') during *'Stage I'* through *'Stage V.*' At *'Stage I,'* the fenders yield entirely and shows average vertical stress of about 2.5 MPa. The fenders formed by splitting the working pillar ('W') show the maximum stress value of about 6 MPa, as seen from Fig. 6.17a. The average vertical stress on the previously extracted pillar is 0.56 MPa. At *'Stage II,'* the first slice has been taken out from the fender, nearby goaf. The remaining portion of the working fender and the next fender show the maximum stress value of about 6 MPa, as seen from Fig. 6.17b. The average vertical stress on the working pillar/remnant ('W') during '*Stage II*' has been observed as 2.38 MPa. The previously

extracted pillar/remnant ('P') shows a negligible change in the stress value at this stage. The average vertical stress on the focused pillars gradually reduces in the subsequent depillaring stages, as seen from Fig. 6.17. The average vertical stress on the working pillar ('W') and the previously extracted pillar ('P') during the last depillaring stage (*'Stage V'*) is 0.46 MPa and 0.43 MPa, respectively.

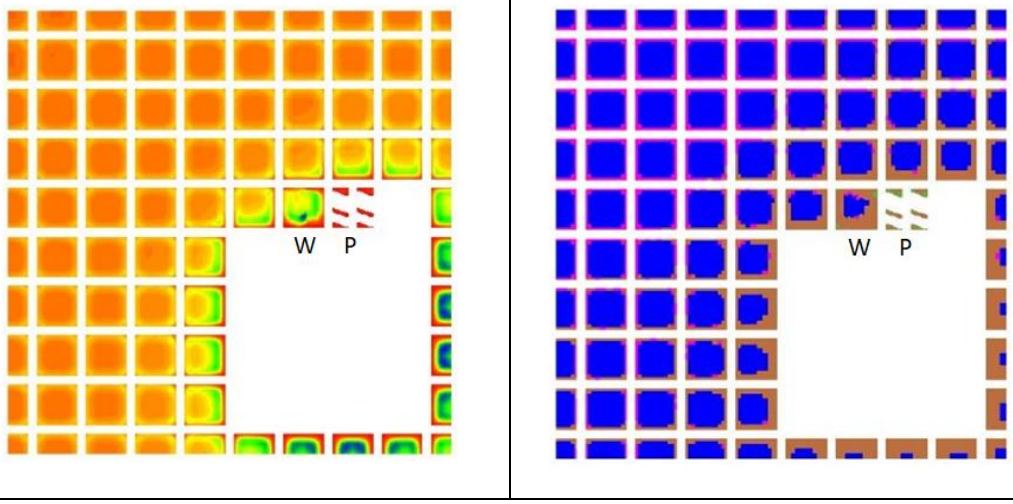

a. Stage 0 (Plan view)

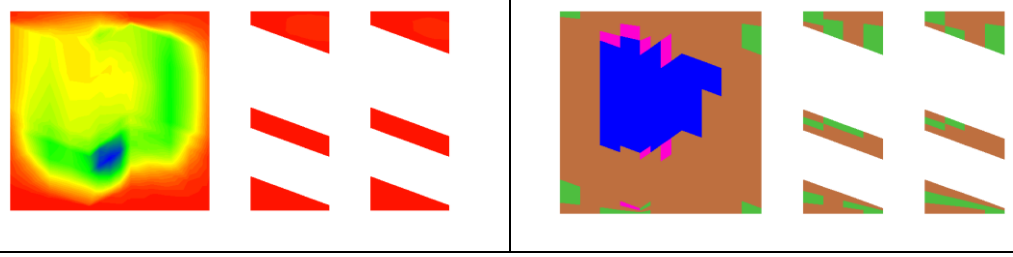

b. Stage 0 (Zoomed view)

Vertical stress scale (stress in Pa)

Yielding state scale

Fig. 6.16 Vertical stress and yield profile of the panel with a pillar width of 35 m and snook width of 4.5 m at a depth of 180m during 'Stage 0'

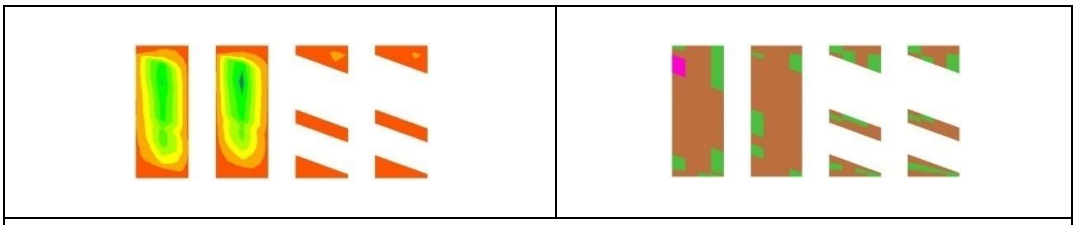

a. Stage I

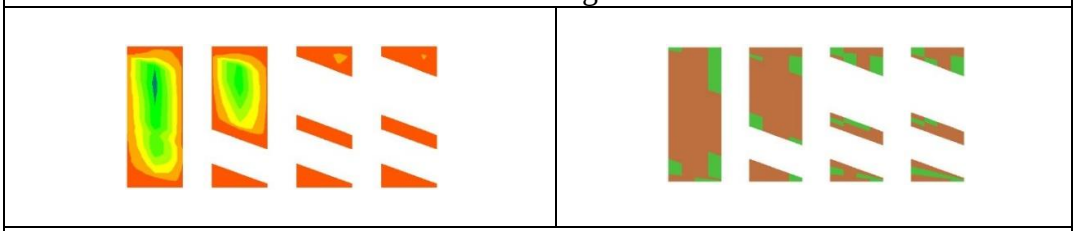

b. Stage II

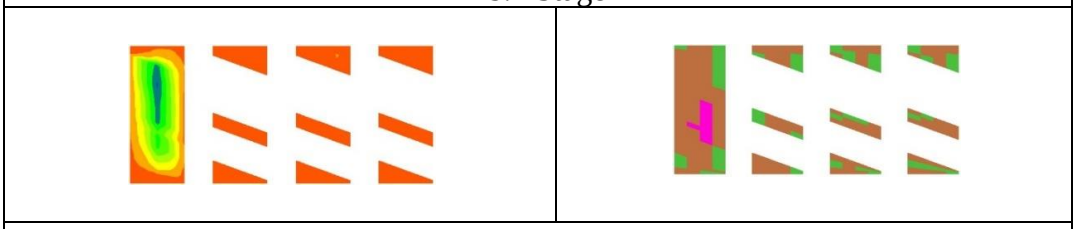

c. Stage III

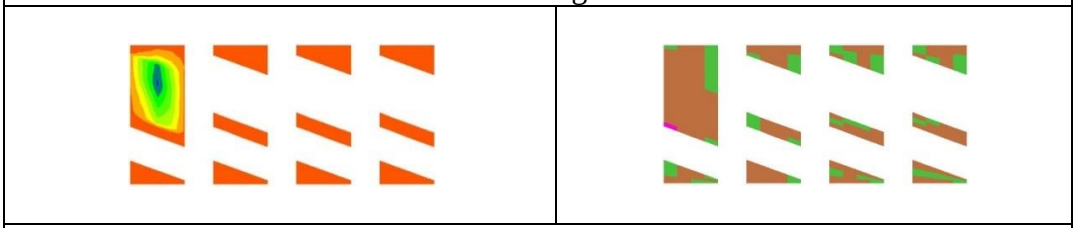

d. Stage IV

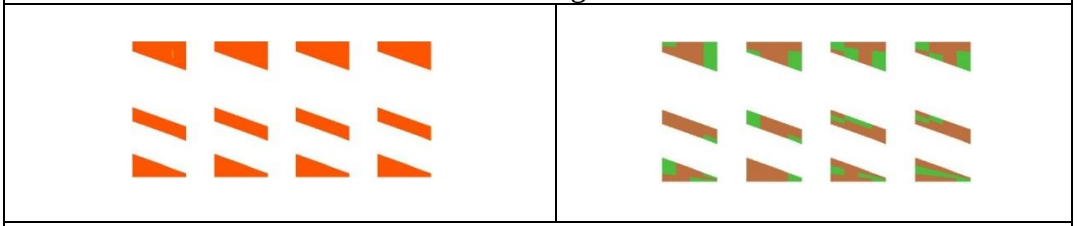

e. Stage V

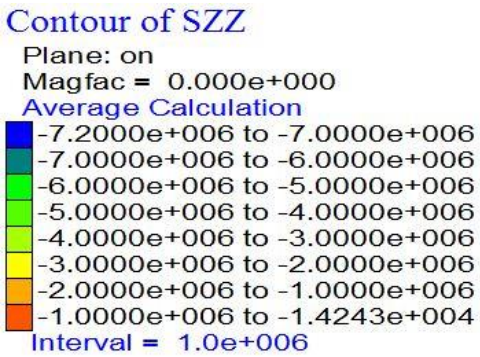

Vertical stress scale (stress in Pa)

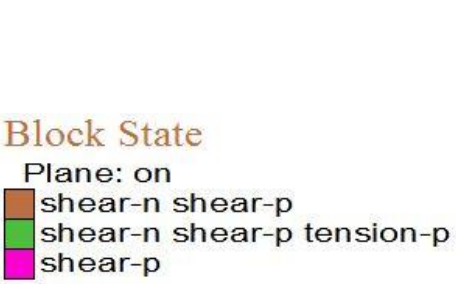

Yielding state scale

Fig. 6.17 Vertical stress and yield profile of the panel with a pillar width of 35 m and snook width of 4.5 m at a depth of 180 m during 'Stage I' through 'Stage V'

The *'Strength Factor* (*SF*) of the concerned pillars/remnants, i.e., working pillar ('W'), and the previously extracted pillar ('P') has been calculated at each stage of depillaring. The weight of the overhang in this scenario is considered as 12,250 T (Eq. 3.2). Table 6.15 shows the simulation results of the panel at six different depillaring stages. The simulation reveals that the working pillar ('W') shows an *SF* value of about 13.6, although the so formed fenders yield completely. The *SF* of the working pillar 'W' and the previously extracted pillar 'P' during the last depillaring stage (*'Stage IV'*) has been calculated as 1.2 and 0.6. Table 6.15 shows the vertical stress and yield percentage of the focused pillars during different depillaring stages.

Table 6.15 Simulation results of remnant pillars for a pillar width of 35 and snook width of 4.5 m at a depth of 180 m

Stage	Previously extracted pillar ('P')			Working pillar ('W')		
	Average Vertical Stress (MPa)	**Yielding (%)**	**SF**	**Average vertical stress (MPa)**	**Yielding (%)**	**SF**
0	0.66	100	1.2	12.54	70	-
1	0.56	100	1.0	2.50	100	13.6
2	0.55	100	1.0	2.38	100	11.3
3	0.51	100	0.9	2.29	100	8.4
4	0.47	100	0.9	1.78	100	5.2
5	0.40	100	0.9	0.65	100	1.2

'-' shows that an intact core is present in the pillar/remnant

6.3.3. Simulation results for pillar width of 45 m

The pillar width of 45 m has been simulated at a depth of 330 m adopting a double split and fender extraction pattern. The working pillar ('W'), and the previously extracted pillar ('P'), have been constructed so that splitting and slicing can be performed at different depillaring stages. The model has been simulated for twelve different depillaring stages (*'Stage 0*' through *'Stage XI'*). The simulation results have

been obtained in terms of vertical stress and yield profile. The dark color (blue) in the vertical stress profile depicts high vertical stress values, whereas the light color (yellow, orange) depicts lower stress values. The load-bearing capacity of the remnant pillars has been determined through the *FISH* function of *FLAC*^{3D}. The '*Strength factor (SF)'* of the concerned pillars/remnants (i.e., 'W' and 'P') has been determined for all the cases of the remnant pillars (i.e., having snook width of 4.5 m, 5.5 m, and 6.5 m). The simulation results of the optimum remnant pillar design satisfying the design criteria have been discussed in this section. The rest cases of the remnant pillar which does not satisfy the design criteria have been provided in the Appendix – C3.

Fig. 6.18 shows the vertical stress and yielding profile of the pillars during *'Stage 0*'. The simulation results show that the maximum vertical stress on the working pillar 'W' is about 93 MPa during '*Stage 0*,' i.e., before the splitting operation. The working pillar ('W') yields about 60% at this stage and shows average vertical stress of about 22.27 MPa. The zoomed view of the focused pillars (i.e., 'W' and 'P') has been shown in Fig. 6.18b. The previously extracted pillar ('P') yields entirely at this stage and shows the average vertical stress of about 0.55 MPa.

Fig. 6.19 shows vertical stress and yield profile of the focused pillars (i.e., 'W' and 'P') during *'Stage I*' through *'Stage IV*.' At *'Stage I,'* the fender formed by splitting the pillar yields entirely, and the maximum vertical stress shifts to the solid portion of the working pillar, as seen from Fig. 6.19a. The working pillar yields about 80% at this stage and shows average vertical stress of about 16.7 MPa. The previously extracted pillar ('P') shows a slight decrement in the average vertical stress, calculated as 0.55 MPa.

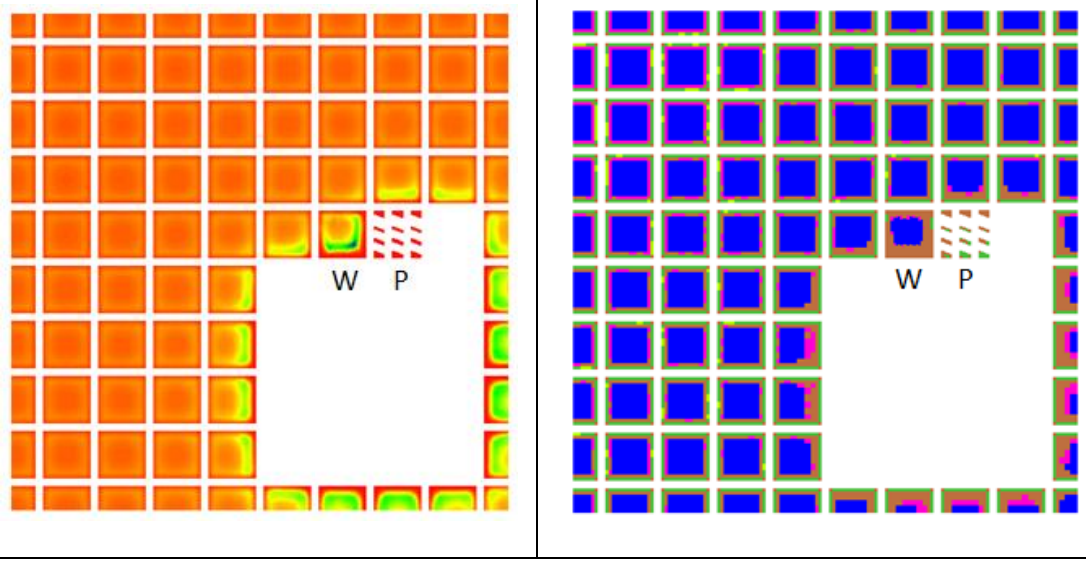

a. Stage 0 (Plan view)

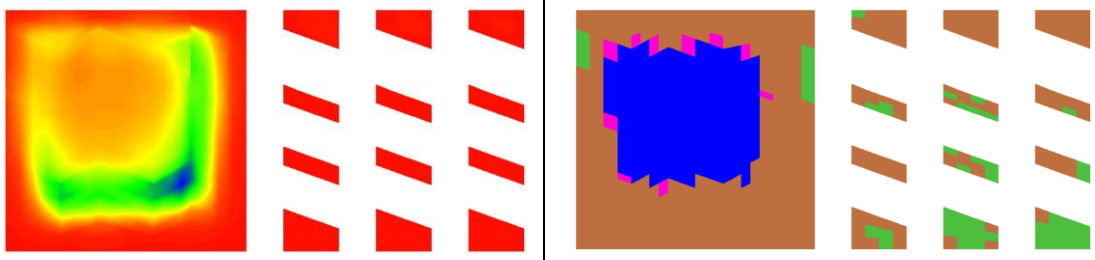

b. Stage 0 (Zoomed view)

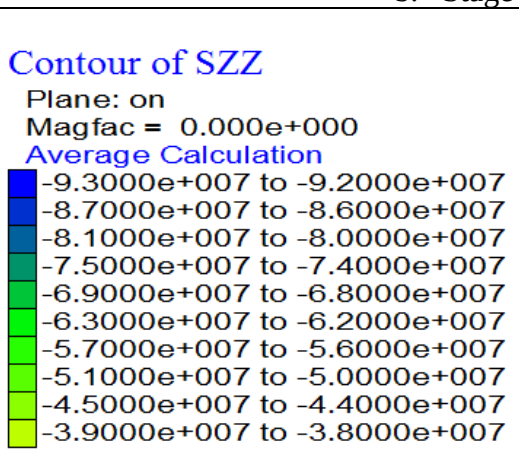

Vertical stress scale (stress in Pa)

Yielding state scale

Fig. 6.18 Vertical stress and yield profile of the panel with a pillar width of 45 m and snook width of 5.5 m at a depth of 330 m during 'Stage 0'

The yield percentage of the working pillars remains the same during *'Stage I'* through *'Stage IV.'* The average vertical stress on the working pillar during '*Stage IV'*

increases to 19.77 MPa. A negligible change in the average vertical stress values has been observed in pillar 'P,' during *'Stage I'* through *'Stage IV'* as seen from Fig. 6.19. The average vertical stress on the previously extracted pillar ('P') during '*Stage IV'* has been observed as 0.49 MPa.

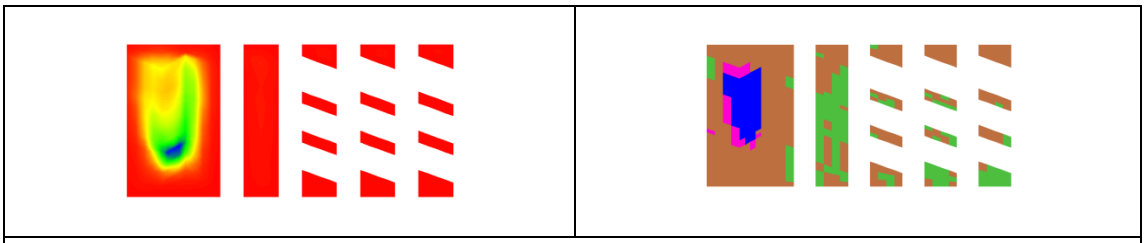

a. Stage I (Zoomed view)

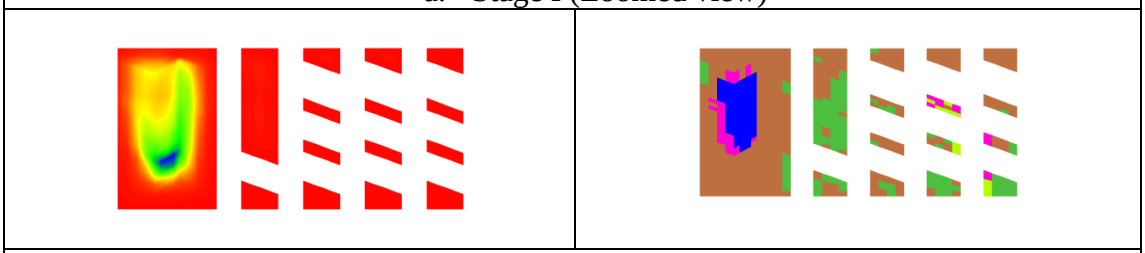

b. Stage II (Zoomed view)

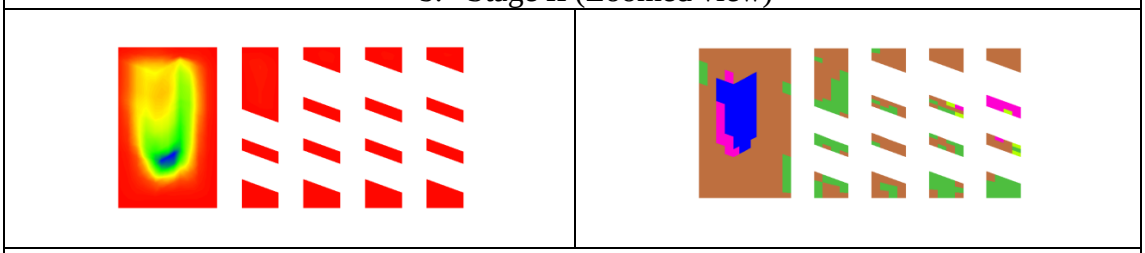

c. Stage III (Zoomed view)

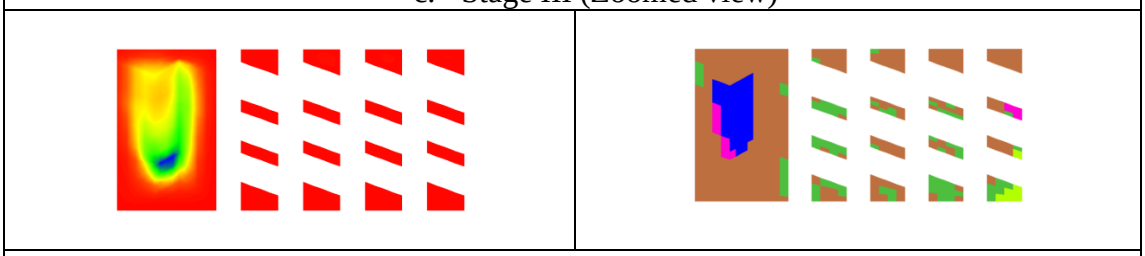

d. Stage IV (Zoomed view)

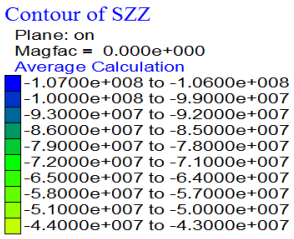

Vertical stress scale (stress in Pa)

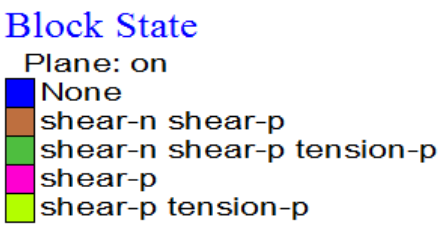

Yielding state scale

Fig. 6.19 Vertical stress and yield profile of the panel with a pillar width of 45 m and snook width of 5.5 m at a depth of 330 m during 'Stage I' through 'Stage IV'

Fig. 6.20 shows vertical stress and yield profile of the focused pillars (i.e., 'W' and 'P') during *'Stage V'* through *'Stage VIII*.' A significant reduction in the vertical stress has been observed in the working pillar ('P') during *'Stage V,*' as seen from Fig. 6.20a. The abutment load shifts to the immediate next pillar at this stage. The newly formed fenders show the maximum stress value of about 35 MPa during '*Stage V*.' The working pillar ('W') ultimately yields at this stage and shows average vertical stress of about 1.12 MPa, as seen in Fig. 6.20. The previously extracted pillar ('P') shows the average vertical stress of about 0.44 MPa during '*Stage V*.' A slight reduction in the average vertical stress values has been observed during *'Stage V'* through *'Stage VIII'* as seen from Fig. 6.20. The maximum vertical stress on the working pillar/remnant ('W') remains the same during these stages, as seen from Fig. 6.20. The average vertical stress on the working pillar and the previously extracted pillar during *'Stage VIII'* was found to be 1.01 MPa, and 0.44 MPa.

Fig. 6.21 shows vertical stress and yield profile of the focused pillar (i.e., 'W' and 'P') during *'Stage IX'* through *'Stage XI*.' The last fender of the working pillar ('W') shows the maximum vertical stress of about 32 MPa during '*Stage IX*,' as seen in Fig. 6.21a. The average vertical stress on the working pillar ('W') reduces to 0.91 MPa at this stage. The previously extracted pillar ('P') shows a negligible change in the average stress value at this stage, as seen in Fig. 6.21. A slight reduction in the average vertical stress values has been observed on the focused pillars (i.e., 'W' and 'P') during the next depillaring stages. The average vertical stress on the working pillar ('W') and the previously extracted pillar during *'Stage XI'* has been observed as 0.49 MPa and 0.44 MPa, respectively.

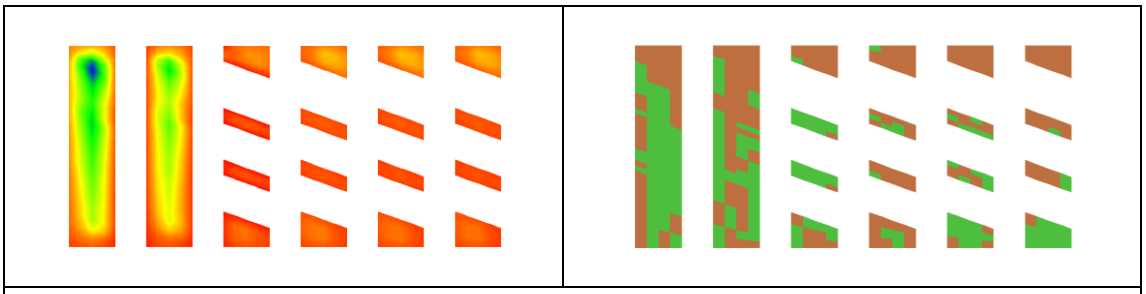

a. Stage V (Zoomed view)

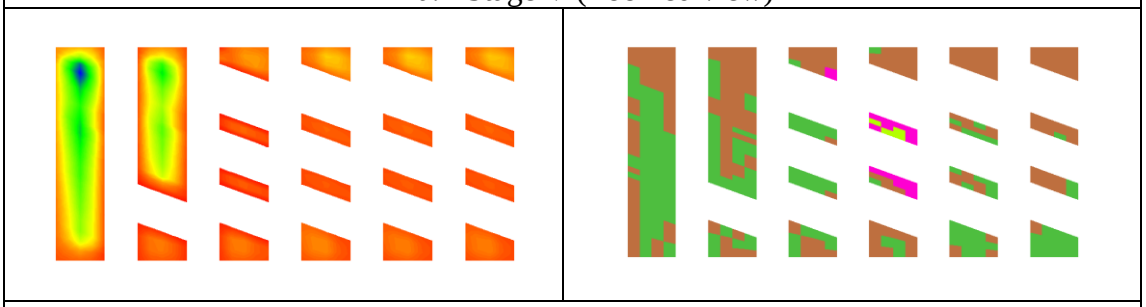

b. Stage VI (Zoomed view)

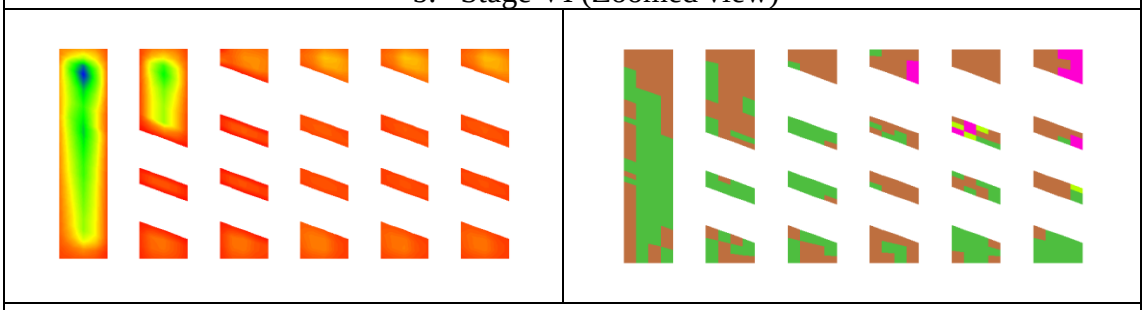

c. Stage VII (Zoomed view)

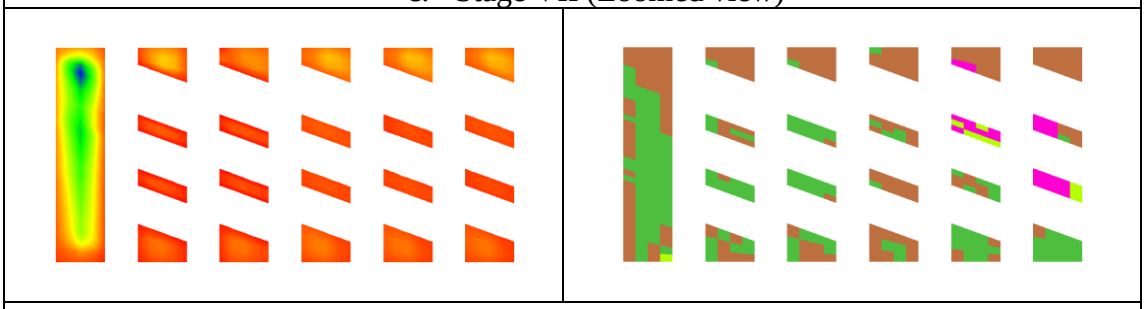

d. Stage VIII (Zoomed view)

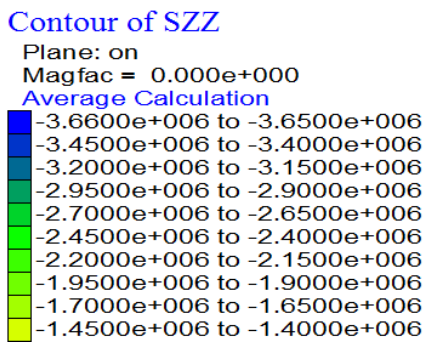

Vertical stress scale (stress in Pa)

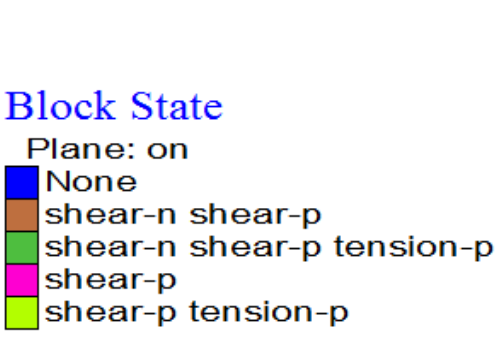

Yielding state scale

Fig. 6.20 Vertical stress and yield profile of the panel with a pillar width of 45 m and snook width of 5.5 m at a depth of 330 m during 'Stage V' through 'Stage VIII'

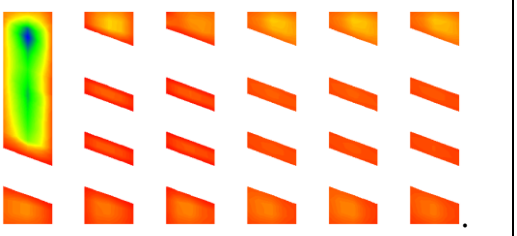

a. Stage IX (Zoomed view)

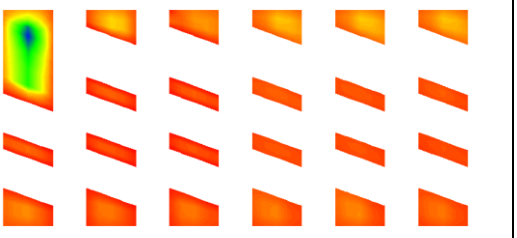

b. Stage X (Zoomed view)

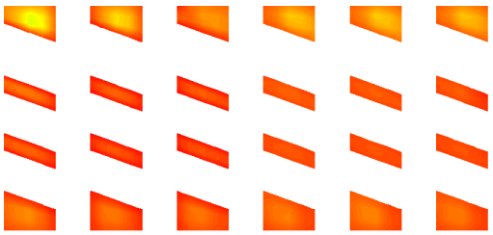

c. Stage XI (Zoomed view)

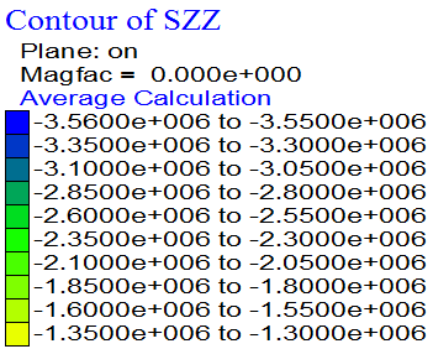

Vertical stress scale (stress in Pa)

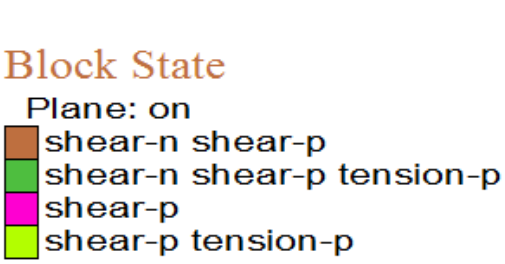

Yielding state scale

Fig. 6.21 Vertical stress and yield profile of the panel with a pillar width of 45 m and snook width of 5.5 m at a depth of 330 m during 'Stage IX' through 'Stage XI'

The *'Strength Factor* (*SF*)' of the concerned pillars/remnants, i.e., the working pillar ('W') and the previously extracted pillar ('P'), have been calculated at each stage of depillaring. The weight of the overhang in this scenario has been calculated as 20,250

tonne (Eq. 3.2). Table 6.16 shows the simulation results of the panel at twelve different depillaring stages. The simulation reveals that the working pillar ('W') yields ultimately during *'Stage V*' and shows an *SF* value of about 4.6. The *SF* of pillar 'W' and pillar 'P' during the last depillaring stage (*'Stage XI'*) has been calculated as 0.9 and 1.0.

Table 6.16 Simulation results of remnant pillars for a pillar width of 45 and snook width of 4.5 m at a depth of 330 m

Stage	**Previously extracted pillar ('P')**			**Working pillar ('W')**		
	Average vertical stress (MPa)	**Yield (%)**	**SF**	**Average vertical stress (MPa)**	**Yield (%)**	**SF**
0	0.55	100	1.1	22.27	60	-
1	0.50	100	1.0	16.70	80	-
2	0.49	100	1.0	17.51	80	-
3	0.50	100	1.0	18.43	80	-
4	0.49	100	1.0	19.77	80	-
5	0.44	100	0.9	1.12	100	4.6
6	0.44	100	0.9	1.12	100	4.2
7	0.44	100	0.9	1.08	100	3.7
8	0.44	100	0.9	1.01	100	3.1
9	0.44	100	0.9	0.91	100	2.5
10	0.44	100	0.9	0.77	100	1.9
11	0.44	100	0.9	0.60	100	1.2

'-' shows that an intact core is present in the pillar/remnant

6.3.4. Simulation results for pillar width of 48 m

The pillar width of 48 m has been simulated at a depth of 420 m adopting a double split and fender extraction pattern. The working pillar ('W'), and the previously extracted pillar ('P'), have been constructed so that splitting and slicing can be performed at different depillaring stages. The model has been simulated for twelve different depillaring stages ('*Stage 0*' through *'Stage XI'*). The simulation results were obtained in terms of vertical stress and yield profile. The dark color (blue) in the

vertical stress profile depicts high vertical stress values, whereas the light color (yellow, orange) depicts lower stress values. The load-bearing capacity of the remnant pillars has been determined through *the FISH* function of *FLAC*^{3D}. The '*Strength factor (SF)'* of the concerned pillars/remnants (i.e., 'W' and 'P') has been determined for all the cases of the remnant pillars (i.e., having snook width of 4.5 m, 5.5 m, and 6.5 m). The simulation results of the optimum remnant pillar design satisfying the design criteria have been discussed in this section. The rest cases of the remnant pillar which does not satisfy the design criteria have been provided in the Appendix – C4.

Fig. 6.22 shows the vertical stress and yielding profile of the pillars during *'Stage 0'*. The working pillar ('W') yields about 70% at this stage and shows average vertical stress of about 27.42 MPa. The maximum vertical stress of about 99 MPa has been observed 7 m – 8 m inside the working pillar ('W'). The zoomed view of the focused pillars (i.e., 'W' and 'P') has been shown in Fig. 6.22b. The previously extracted pillar yields entirely at *'Stage 0*' and shows the average vertical stress of about 0.67 MPa.

Fig. 6.23 shows vertical stress and yield profile of the focused pillar (i.e., 'W' and 'P') during *'Stage I*' through *'Stage IV*.' The working pillar yields about 90% during *'Stage I*' and shows average vertical stress of about 11.66 MPa. The fender of the working pillar (towards goaf) shows complete yielding at this stage. The previously extracted pillar ('P') shows a slight decrement in the average vertical stress, calculated as 0.53 MPa. A slight increment in the average vertical stress values has been observed in pillar 'W,' during *'Stage I*' through *'Stage IV'* as seen in Fig. 6.23. The yield percentage of the working pillars remains the same during these stages, as seen from Fig. 6.23. The average vertical stress on the working pillar and the previously extracted pillar during '*Stage IV'* has been obtained as 13.71 MPa, and 0.52 MPa.

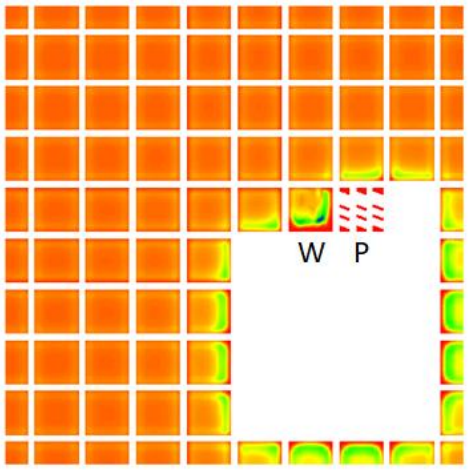

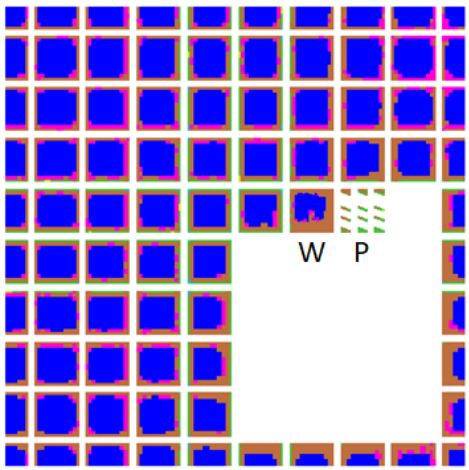

a. Stage 0 (Plan view)

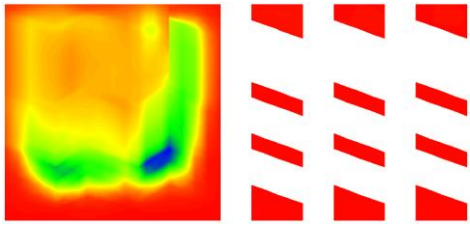

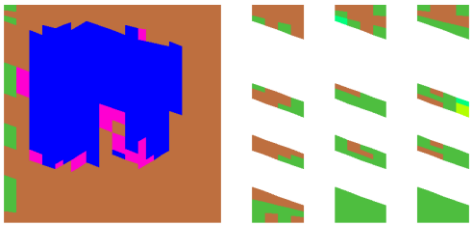

b. Stage 0 (Zoomed view)

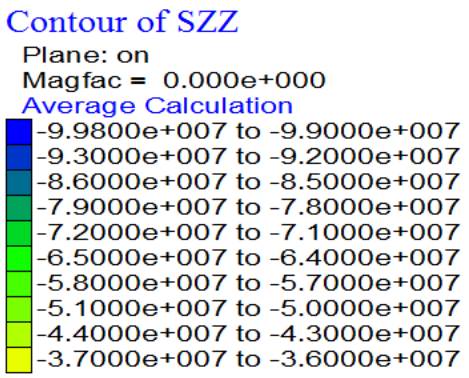

Vertical stress scale (stress in Pa)

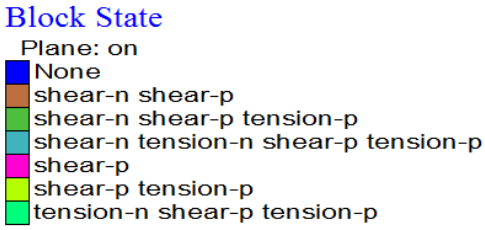

Yielding state scale

Fig. 6.22 Vertical stress and yield profile of the panel with a pillar width of 48 m and snook width of 5.5 m at a depth of 420 m during 'Stage 0'

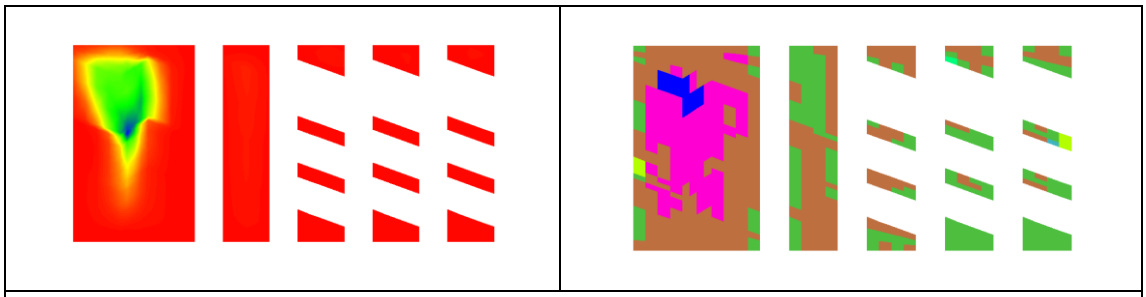

a. Stage I (Zoomed view)

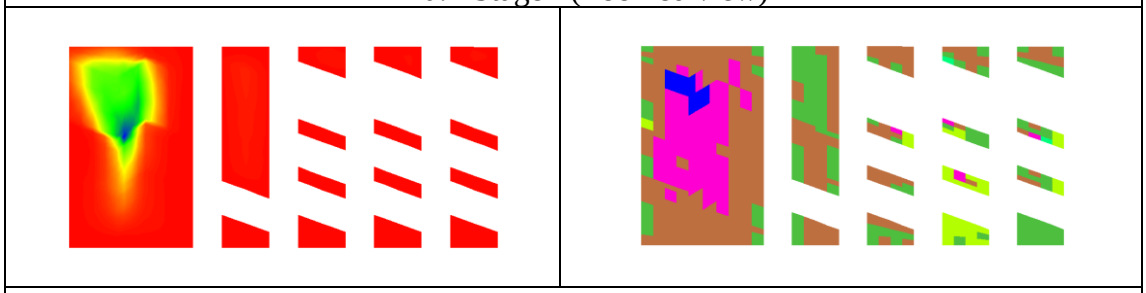

b. Stage II (Zoomed view)

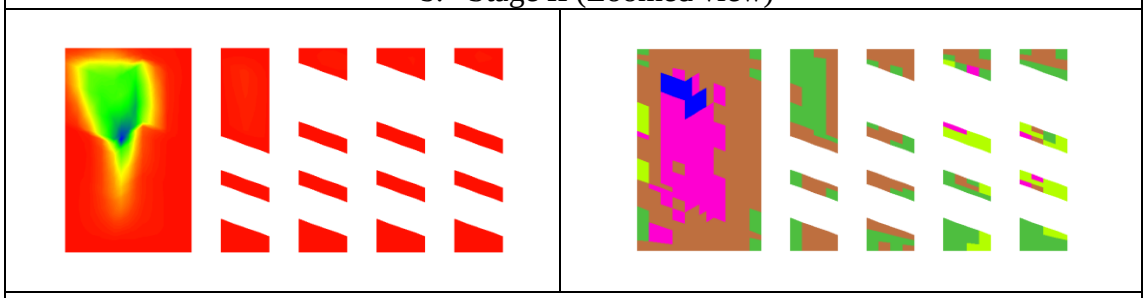

c. Stage III (Zoomed view)

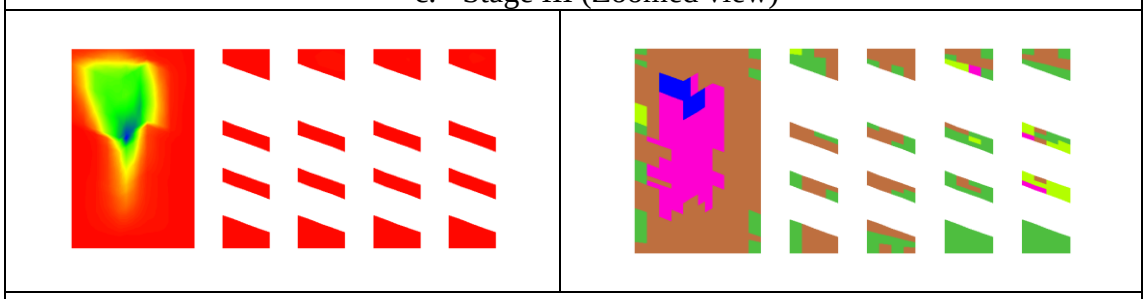

d. Stage IV (Zoomed view)

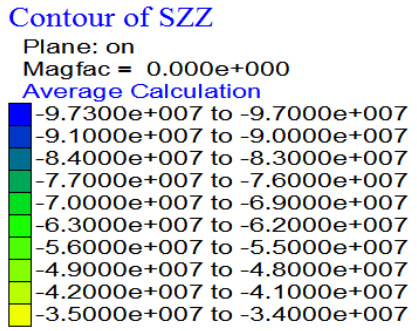

Vertical stress scale (stress in Pa)

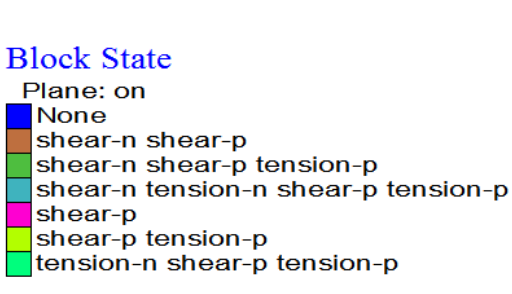

Yielding state scale

Fig. 6.23 Vertical stress and yield profile of the panel with a pillar width of 48 m and snook width of 5.5 m at a depth of 420 m during 'Stage I' through 'Stage IV'

Fig. 6.24 shows vertical stress and yield profile of the focused pillar (i.e., Pillar ‘W’ and ‘P’) during *'Stage V*' through *'Stage VIII*.' A significant reduction in the vertical stress has been observed in the working pillar ‘W’ during ‘*Stage V*,’ as seen from Fig. 6.24a. The abutment load shifts to the next solid pillar, and the maximum stress on the newly formed fender has been observed as 33 MPa. The working pillar ‘W’ ultimately yields at this stage and shows the average vertical stress of about 1.08 MPa. The previously extracted pillar 'P' shows average vertical stress of about 0.47 MPa during ‘*Stage V*.’ A minor change in the average vertical stress values has been observed during *'Stage V*' through *'Stage VIII'* as seen from Fig. 6.24. The average vertical stress on the working pillar ‘W’ and the previously extracted pillar ‘P’ during *'Stage VIII*' was found to be 0.99 MPa and 0.45 MPa.

Fig. 6.25 shows vertical stress and yield profile of the focused pillar (i.e., ‘W’ and ‘P’) during *'Stage IX'* through *'Stage XI*.' The average vertical stress of the working pillar ‘W’ reduces to 0.93 MPa during ‘*Stage IX*.’ The previously extracted pillar ‘P’ shows a negligible change in the average vertical stress at this stage. A slight reduction in the average vertical stress values has been observed in the next depillaring stages, as seen in Fig. 6.25. The average vertical stress on the working pillar ‘W’ during *'Stage XI'* has been observed as 0.49 MPa. The average vertical stress on the previously extracted pillar ‘P’ at this stage has been obtained as 0.46 MPa.

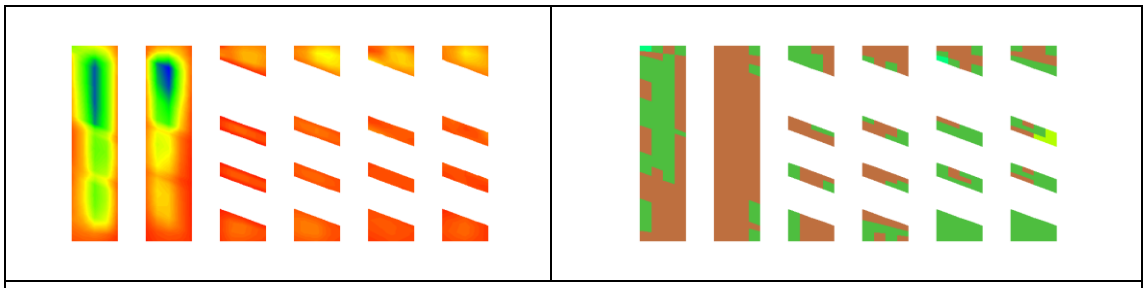

a. Stage V (Zoomed view)

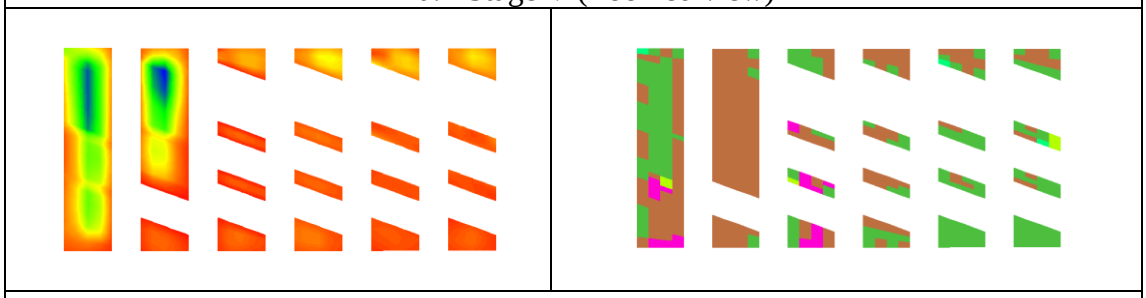

b. Stage VI (Zoomed view)

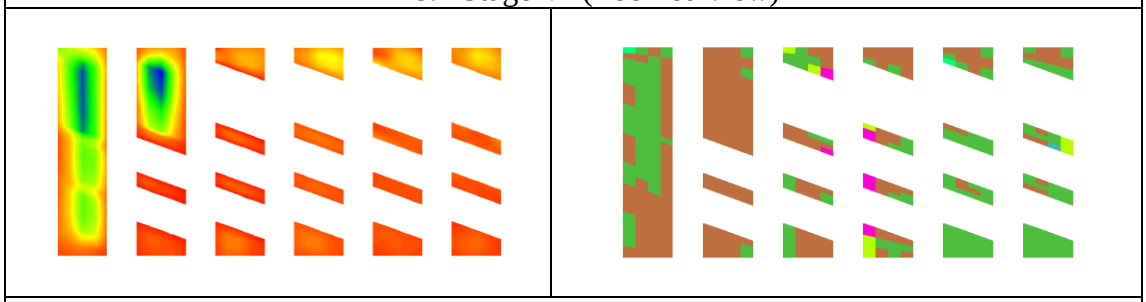

c. Stage VII (Zoomed view)

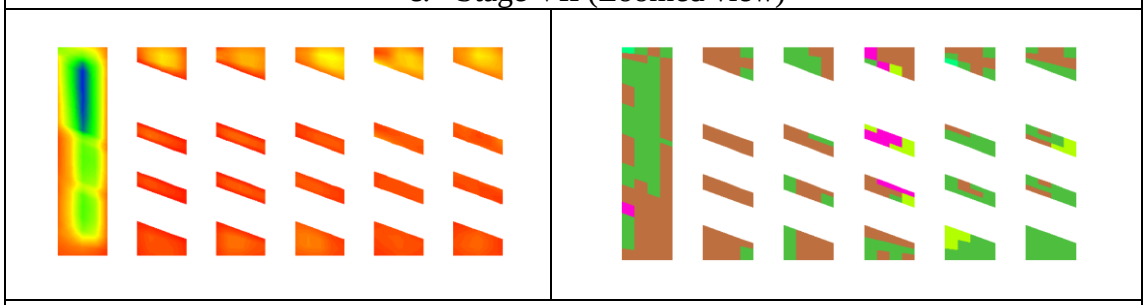

d. Stage VIII (Zoomed view)

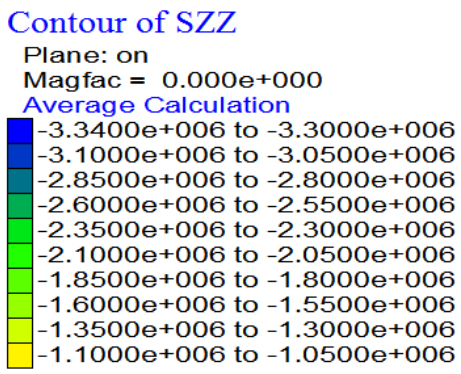

Vertical stress scale (stress in Pa)

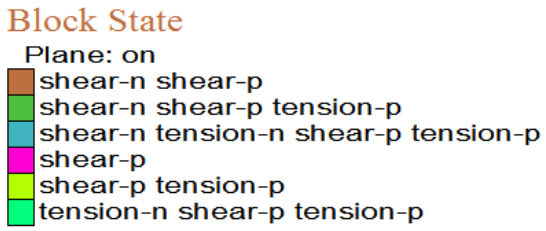

Yielding state scale

Fig. 6.24 Vertical stress and yield profile of the panel with a pillar width of 48 m and snook width of 5.5 m at a depth of 420 m during 'Stage V' through 'Stage VIII'

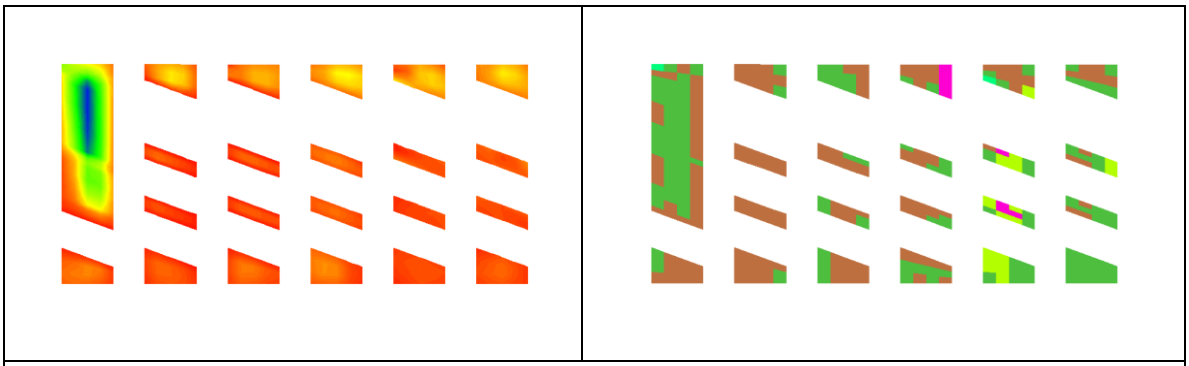

a. Stage IX (Zoomed view)

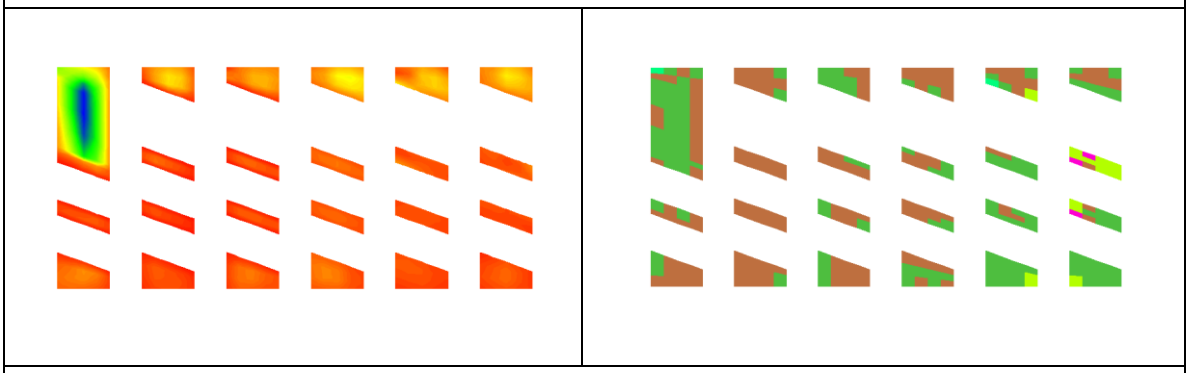

b. Stage X (Zoomed view)

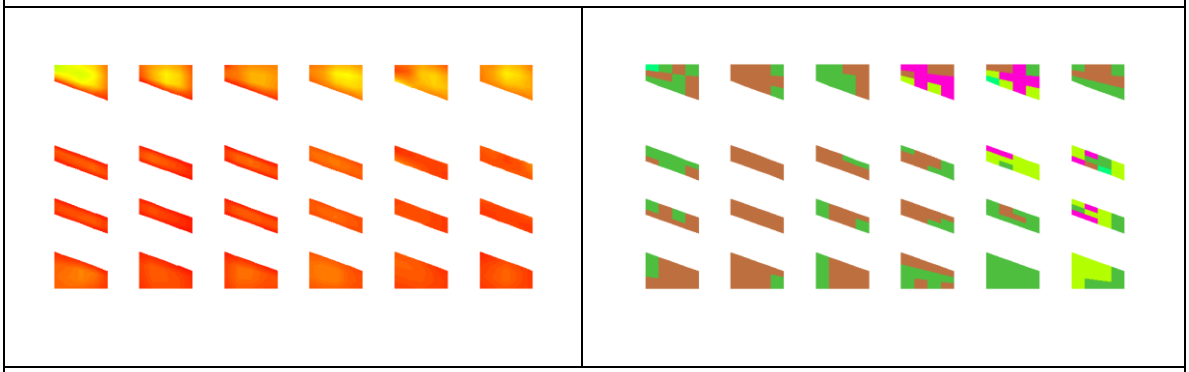

c. Stage XI (Zoomed view)

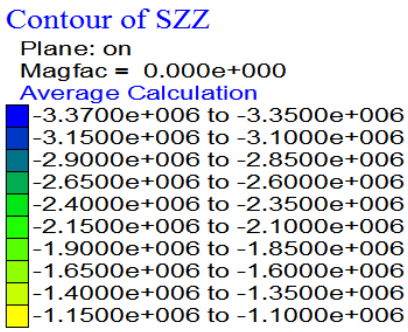

Vertical stress scale (stress in Pa)

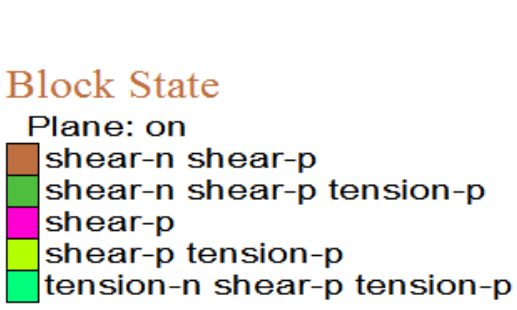

Yielding state scale

Fig. 6.25 Vertical stress and yield profile of the panel with a pillar width of 48 m and snook width of 5.5 m at a depth of 420 m during 'Stage IX' through 'Stage XI'

The *'Strength Factor* (*SF*)' of the concerned pillars/remnants, i.e., the working pillar ('W') and the previously extracted pillar ('P'), have been calculated at each stage of depillaring. The weight of the overhang in this scenario has been calculated as 23,040 T (Eq. 3.2). Table 6.17 shows the simulation results of the panel at twelve different depillaring stages. The simulation reveals that the working pillar ('W') yields ultimately during *'Stage V'* and shows an *SF* value of about 4.7. The *SF* of the working pillar 'W' and the previously extracted pillar 'P' during the last depillaring stage (*'Stage XI'*) has been calculated as 0.9 and 1.0.

Table 6.17 Simulation results of remnant pillars for a pillar width of 48 m and snook width of 5.5 m at a depth of 420 m

Stage	**Previously extracted pillar ('P')**			**Working pillar ('W')**		
	Average vertical stress (MPa)	**Yield (%)**	**SF**	**Average vertical stress (MPa)**	**Yield (%)**	**SF**
0	0.67	100	1.4	27.42	70	-
1	0.53	100	1.1	11.66	90	-
2	0.52	100	1.1	12.17	90	-
3	0.52	100	1.1	12.67	90	-
4	0.52	100	1.1	13.71	90	-
5	0.47	100	1.0	1.08	100	4.7
6	0.47	100	1.0	1.10	100	4.4
7	0.47	100	1.0	1.10	100	4.1
8	0.45	100	0.9	0.99	100	3.2
9	0.46	100	0.9	0.93	100	2.7
10	0.46	100	0.9	0.86	100	2.2
11	0.46	100	0.9	0.52	100	1.1

6.3.5. Analysis for remnant pillar design

The remnant pillars (ribs/snook) are the critical elements of a mechanized depillaring panel and play an essential role in restricting goaf encroachment in the working area. The remnant pillars are formed during final coal extraction, adopting a suitable extraction pattern. Fish-bone, and split and fender are the commonly used patterns adopted for small (less than generally 30 m) and large (greater than generally 30 m)

pillars. The design of the remnant pillars mainly governs the local stability in the panel. An attempt has been made in the study to design the remnant pillar for each selected pillars (i.e., having pillar width of 26 m, 35 m, 45 m, and 48 m) using numerical techniques. The fish-bone extraction pattern has been considered for pillar width of 26 m and split and fender pattern for pillar width of 35 m. The pillar width of 45 m and 48 m has been extracted using a double split and fender pattern. The optimum remnant pillar design is considered to be the one satisfying the design criteria, which states that the *SF* of the working pillar ('W') should not be less than 1.0 until the last slice has been taken out from the pillar ('W'), and at that depillaring stage the *SF* of the previously extracted pillar ('P') should be less than 1.0. Numerical models were prepared for a complete panel (including remnant pillars) and simulated at a critical depillaring stage and critical depth. The remnant pillar design has been optimized in the study by varying the size of the final snook. Three different snook widths (i.e., 4.5 m, 5.5 m, and 6.5 m) have been chosen for the study. The simulation results of the optimum case of the remnant pillars for each selected intact pillar have been discussed in Section 6.3.1 through Section 6.3.4. The simulation results of the last depillaring stage for each selected pillars (i.e., having pillar width of 26 m, 35 m, 45 m, and 48 m) have been chosen for the analysis, as shown in Table 6.18 through Table 6.21. The *SF* of the remnant pillars has been calculated for each combination of the selected pillar and snook width. The overhang weight has been calculated using Eq. 6.2, considering the overhang area equivalent to a pillar size and thickness as 4.0 m. The density of the immediate strata has been considered as 2.5 g/cm^2. The reaction provided by the remnant pillar has been obtained using the *FISH* function of *FLAC^{3D}*.

Table 6.18 *SF* of the focused remnant pillars for pillar width of 26 m

Pillar width (m)	Snook width (m)	Area (m2)	Overhang load (MN)	Reaction(MN)		SF	
				Remnant P	Remnant W	Remnant P	Remnant W
26	4.5	130	68	42	87	0.6	1.3
26	5.5	135	68	46	93	0.7	1.4
26	6.5	142	68	67	122	1.0	1.8

Table 6.19 *SF* of the focused remnant pillars for pillar width of 35 m

Pillar width (m)	Snook width (m)	Area (m2)	Overhang load (MN)	Reaction (MN)		SF	
				Remnant P	Remnant W	Remnant P	Remnant W
35	4.5	228	123	97	148	0.8	1.2
35	5.5	251	123	142	150	1.2	1.2
35	6.5	273	123	163	167	1.3	1.4

Table 6.20 SF of the focused remnant pillars for pillar width of 45 m

Pillar width (m)	Snook width (m)	Area (m2)	Overhang load (MN)	Reaction (MN)		SF	
				Remnant P	Remnant W	Remnant P	Remnant W
45	4.5	404	203	179	196	0.8	1.0
45	5.5	431	203	189	238	0.9	1.2
45	6.5	457	203	244	269	1.2	1.3

Table 6.21 SF of the focused remnant pillars for pillar width of 48 m

Pillar width (m)	Snook width (m)	Area (m2)	Overhang load (MN)	Reaction (MN)		SF	
				Remnant P	Remnant W	Remnant P	Remnant W
48	4.5	*444*	230	180	200	0.8	0.9
48	5.5	475	230	217	243	0.9	1.1
48	6.5	507	230	278	289	1.2	1.3

The optimum remnant pillar design is considered to be the one satisfying the design criteria. Fig. 6.26 shows the graphical representation of the optimum remnant pillar design for each selected pillar. It has been depicted from Fig. 6.26 that the *SF* of the working remnant pillar ('P') is above 1.0, and the *SF* of the previously extracted pillar is less than 1.0. The analysis of the simulation results shows that the case of remnant pillar having a snook width of 4.5 m satisfies the design criteria for a pillar width of

26 m and 35 m, whereas the optimum remnant pillar design for pillar width of 45 m and 48 m has been observed to be the one with snook width of 5.5 m.

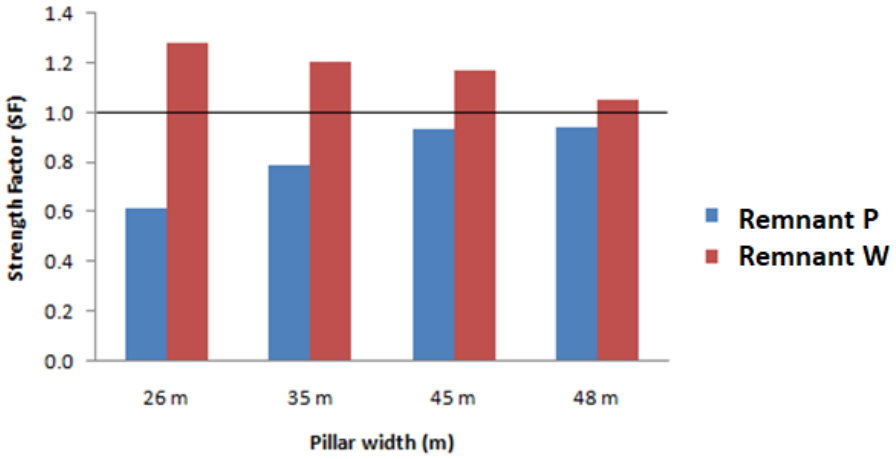

Fig. 6.26 Graphical representation of the SF of the remnant pillars for the selected pillars

Table 6.22 shows the simulation results of the optimum cases of the remnant pillars for each selected pillar. It has been observed from the analysis that the optimum area of remnant pillar for pillar width of 26 m is about 130 m^2, whereas for pillar width of 35 m, 45 m, and 48 m, the optimum remnant pillar area has been obtained as 228 m^2, 431 m^2, and 475 m^2, respectively. The *SF* of the optimum remnant pillars for each selected pillar have been shown in Table 6.22.

Table 6.22 *SF* of the optimum remnant pillar design for the selected pillars

Pillar width (m)	Area of remnant (m2)	Overhang load (MN)	Reaction (MN)		SF	
			Remnant P	Remnant W	Remnant P	Remnant W
26	130	68	42	87	0.6	1.3
35	228	123	97	148	0.8	1.2
45	431	203	189	238	0.9	1.2
48	475	230	217	243	0.9	1.1

Based on numerical simulation results, a graph has been plotted (fig. 6.27) in between the reaction provided by the remnant pillar vis-à-vis its area. The graph shows an

exponential relationship as expressed in Eq. 6.4. One can determine the load-bearing capacity of the remnant pillars using Eq. 6.4.

$$L = 54.51\ x\ e^{(0.003\ x\ A)} \qquad (6.4)$$

Where L is the Load-bearing capacity of the remnant pillar in kT, and A is the area of the remnant pillar in m^2

The average vertical stress on the focused remnant pillars (i.e., Remnant pillar 'W,' and 'P') has also been determined for the optimum cases. The average vertical stress on the working remnant pillar 'W' lies in the range of 0.51 MPa – 0.67 MPa. The previously extracted pillar 'P' shows average vertical stress in the range of 0.32 – 0.46 MPa. Table 6.23 shows the average vertical stress on the focused remnant pillars (i.e., remnant pillar ‘W’ and ‘P’).

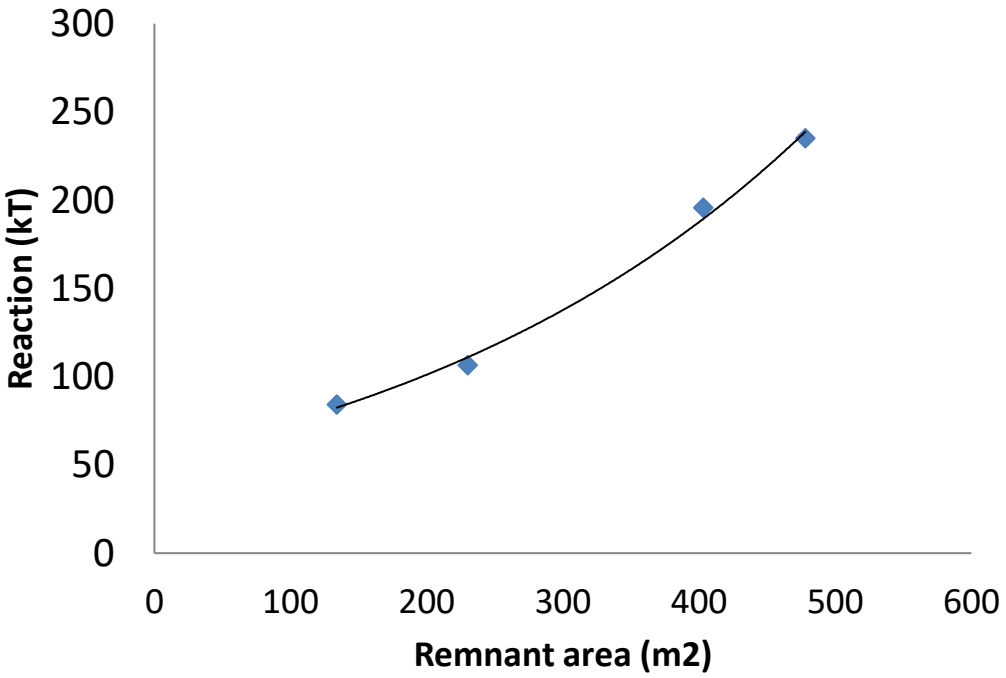

Fig. 6.27 Graph showing reaction provided by the remnant pillar for different areas

Table 6.23 Average vertical stress on the focused remnant pillars for the selected pillars

Pillar width (m)	Remnant area (m2)	Average vertical stress (MPa)	
		Remnant P	Remnant W
26	130	0.32	0.67
35	228	0.42	0.65
45	431	0.44	0.55
48	475	0.46	0.51

Based on the analysis, a relationship has been developed to design the remnant pillars.

$$\frac{L_P}{0.4\ x\ A} < 1.0 \qquad (6.5)$$

$$\frac{L_W}{0.6\ x\ A} > 1.0 \qquad (6.6)$$

Where L_P is load-bearing capacity of the previously extracted remnant pillar ('P'), L_W is load-bearing capacity of the working remnant pillar ('W'), and A is the area of remnant pillars.

The simulation results have been further analyzed to determine the percentage of the extraction in the optimum cases of the remnant pillars. Table 6.24 shows the percentage of extraction for each selected pillars with optimum remnant pillar design. The analysis shows that the extraction percentage should not exceed 80% for safe depillaring operation. One can determine the optimum area of remnant pillar for different pillar widths considering 80% extraction and then adjusting the area to satisfy Eq. 6.5 and Eq. 6.6.

Table 6.24 Percentage of extraction in optimum cases of remnant pillars for the selected pillars

Pillar width (m)	Remnant area (m2)	Extraction % w.r.t. Pillar width (Center to center)
26	130	80.77
35	228	81.39
45	431	78.72
48	475	79.38

The optimum cases of the remnant pillars have been further analyzed to access the size of the snook. The area of the snook in the optimum cases of the remnant pillars for each selected pillars has been determined in the study using *FISH* function of *FLAC*^{3D}. Table 6.25 shows the optimum area of snook for the selected pillars and their respective percentages. It has been analyzed from the simulation results that the snook is about 5% of the pillar area for smaller pillars, and about 8% for larger pillars.

Table 6.25 Optimum area and percentage of the snook for different pillar sizes

Pillar width (m)	**Snook area (m2)**	**Snook%**
26	31.5	4.7
35	103.5	8.4
45	148.5	7.3
48	165	7.2

6.3.6. Guidelines for remnant pillar design

The intact pillars and remnant pillars (ribs/snook) are the critical elements of a mechanized depillaring panel. The stability of the pillars mainly governs the global stability in the panel, whereas the role of a remnant pillar is to provide temporary support to the strata. The remnant pillar design requirement is that it bears the overhang load until last has been taken out from the pillar and fails after depillaring advances to a safe distance. The *'Strength factor (SF)'* has been used in the study to assess the stability of the remnant pillars. The SF is the ratio of the residual strength of the remnant pillars and the weight of the overhang. The optimum remnant pillar design is considered to be the one in which the *SF* of the working pillar/remnant 'W' is greater than 1.0 while taking the last slice from the pillar, and at that stage, the *SF* of the previously extracted pillar/remnant 'P' should be less than 1.0. An expression

has been derived in the study to determine the load-bearing capacity of the remnant pillar based on its area (Eq. 6.4). One can design the remnant pillars using Eq. 6.5 and Eq. 6.6. An illustration has been provided in the study to design the remnant pillars for a mechanized depillaring panel.

Illustration 6.2: Remnant pillar design during mechanized depillaring

The steps to be followed for designing the remnant pillar have been given below:

Step 1: Select the pillar width (center to center).

Let the width of the pillar be 38 m.

Step 2: Calculate the expected area of the remnant pillars considering 80% extraction.

$$\text{Expected area of remnant pillars} = (38\ x\ 38) - \left(\frac{80}{100}\right) x\ (38\ x\ 38)$$

$$\text{Expected area of remnant pillars} = 288.8\ m^2$$

Step 3: Calculate the load of the immediate strata using Eq. 3.2, considering the density of immediate strata as 2.3 g/cm^3, the thickness of immediate strata as 4.0 m, and the area of the overhang equivalent to the pillar size.

$$\text{Load of the immediate strata } = 2.3\ x\ 38\ x\ 38\ x\ 4.0$$

$$= 13284.8\ T$$

Step 4: Calculate the load bearing capacity of the focused remnant pillars (i.e., Remnant pillar 'W,' and 'P') using Eq. 6.5 and Eq. 6.6

For remnant pillar 'W,'

$$\text{Load bearing capcity } (' \text{W}') = 0.6x\ 288.8$$

$$= 173.28\ MPa$$

Or,

$$\text{Load bearing capcity } (' \text{W}') = 17328\ T$$

For remnant pillar 'P,'

$$\text{Load bearing capcity } (' \text{P}') = 0.4x\ 288.8$$

$$= 115.52\ MPa$$

Or,

$$\text{Load bearing capcity } (' \text{P}') = 11552\ T$$

Step 5: Calculate the *SF* for focused remnant pillars, i.e., remnant pillar 'W,' and 'P,' using Eq. 6.5 and Eq. 6.6.

For remnant pillar 'W,'

$$SF_W = \frac{17328}{13284.8}$$

$$SF_W = 1.3$$

For remnant pillar 'P,'

$$SF_P = \frac{11552}{13284.8}$$

$$SF_P = 0.87$$

Step 5: If *SF* for remnant pillar 'W,' and 'P' satisfy the design criteria (i.e., SF of remnant pillar 'W' should be greater than 1.0, and SF of remnant pillar 'P' should be less than 1.0), then the selected area of the remnant pillar is the optimum one, else adjust the area of the remnant pillar by varying the extraction percentage and repeat the same exercise from '*Step 2*.'

Note: Once the optimum area of the remnant pillar has been determined, one can design the snook by considering the width of the in-bye rib (left before slicing the pillar/fender) as 5.0 m and the width of the in-between (left between two or three consecutive slices) as 3.0 m.

6.4.Concluding remarks

The intact pillars and remnant pillars (ribs/snook) are the key elements of a depillaring panel. An attempt has been made in the study to design the bord and pillar panel for mechanized depillaring using numerical techniques. The study has been carried out in two phases, i.e., a) Designing the panel (including working and barrier pillars) and b) Designing the remnant pillars. Numerical models of a sufficiently large panel have been prepared in the study and simulation results have been obtained in terms of vertical stress and yield profiles. The guidelines have been prepared from the analysis to design the pillars for a mechanized depillaring panel. A nomograph has also been prepared in the study depicting the optimum width of pillar for different depths of cover and extraction heights (considering the UCS of coal as 40 MPa). The remnant pillar designing exercise has been carried out by simulating the panel with each selected pillars (i.e., having pillar width of 26 m, 35 m, 45 m, and 48 m) at a critical depth of cover (as determined from the panel design exercise). The term '*Strength factor (SF)'* has been coined to assess the stability of the remnant pillars during depillaring. An expression has been developed to determine the load-bearing capacity of the remnant pillar based on its area. A generalized expression has also been developed to determine the *SF* of the remnant pillars. The analysis of the simulation results shows that the snook is about 5% of the pillar area for smaller pillar and about 8% for larger pillars. Guidelines have been provided in the study to design the remnant pillars for a mechanized depillaring panel.